THE JOURNAL OF COMPARATIVE NEUROLOGY 508:72–93 (2008)

Neuronal and Glial Localization of α_{2A}-Adrenoceptors in the Adult Zebrafish (*Danio rerio*) Brain

KONSTANTINOS AMPATZIS,[1] MARIA KENTOURI,[1] AND CATHERINE R. DERMON[2]*
[1]Biology Department, University of Crete, 71409 Heraklion, Crete, Greece
[2]Biology Department, University of Patras, 26500 Rion, Greece

ABSTRACT

The α_{2A}-adrenoceptor (AR) subtype, a G protein-coupled receptor located both pre- and postsynaptically, mediates adrenaline/noradrenaline functions. The present study aimed to determine the α_{2A}-AR distribution in the adult zebrafish (*Danio rerio*) brain by means of immunocytochemistry. Detailed mapping showed labeling of α_{2A}-ARs, in neuropil, neuronal somata and fibers, glial processes, and blood vessels. A high density of α_{2A}-AR immunoreactivity was found in the ventral telencephalic area, preoptic, pretectal, hypothalamic areas, torus semicircularis, oculomotor nucleus (NIII), locus coreruleus (LC), medial raphe, medial octavolateralis nucleus (MON), magnocellular octaval nucleus (MaON), reticular formation (SRF, IMRF, IRF), rhombencephalic nerves and roots (DV, V, VII, VIII, X), and cerebellar Purkinje cell layer. Moderate levels of α_{2A}-ARs were observed in the medial and central zone nuclei of dorsal telencephalic area, in the periventricular gray zone of optic tectum, in the dorsomedial part of optic tectum layers, and in the molecular and granular layers of all cerebellum subdivisions. Glial processes were found to express α_{2A}-ARs in rhombencephalon, intermingled with neuronal fibers. Medium-sized neurons were labeled in telencephalic, diencephalic, and mesencephlic areas, whereas densely labeled large neurons were found in rhombencephalon, locus coeruleus, reticular formation, oculomotor area, medial octavolateralis and magnocellular octaval nuclei, and Purkinje cell somata. The functional role of α_{2A}-ARs on neurons and glial processes is not known at present; however, their strong relation to the ventricular system, somatosensory nuclei, and nerves supports a possible regulatory role of α_{2A}-ARs in autonomic functions, nerve output, and sensory integration in adult zebrafish brain. J. Comp. Neurol. 508:72–93, 2008.

Indexing terms: catecholamines; hypothalamus; locus coeruleus; nerves; noradrenergic receptors; teleost fish

Noradrenaline (NA; norepinephrine) is an important neurotransmitter in both the peripheral and the central nervous systems (CNS) and an essential regulator of nervous system development in vertebrates. In teleosts, catecholamines serve a variety of central and peripheral functions (Santer, 1977; Randall and Perry, 1992) and influence social and agonistic behavior (Marrone et al., 1966; Maler and Ellis, 1987; Nechaev, 1991; Winberg and Nilsson, 1992, 1993), courtship (Maler and Ellis, 1987), and reproductive behavior (Peter and Fryer, 1983). The noradrenergic neurons of the locus coeruleus (LC) have wide projections throughout the brain neuraxis (Smeets and Gonzales, 2000), and norepinephrine functions are mediated by three main types of adrenoceptors (ARs) α_1-AR, α_2-AR, and β-AR (Bylund et al., 1994; Bylund, 2005) that are part of the superfamily of G protein-coupled receptors (GPCRs; Docherty, 1998). In mammals, it is established that the α_2-ARs include three well-characterized receptor subtypes, α_{2A}-, α_{2B}-, and α_{2C}-AR (Bylund, 1988; Lorenz et al., 1990; Harrison et al., 1991; Scheinin et al., 1994; Docherty, 1998; Civantos Calzada and Aleixandre de Artiñano, 2001).

Grant sponsor: European Social Fund and National Resources (EPEAEK II–PYTHAGORAS I); Grant number: 1942; Grant sponsor: University of Patras (CARATHEODORY); Grant number: C-170.

*Correspondence to: Catherine R. Dermon, Human and Animal Physiology Laboratory, Biology Department, University of Patras, 26500 Rio, Greece. E-mail: dermon@upatras.gr or dermon@biology.uoc.gr

Received 30 March 2007; Revised 27 July 2007; Accepted 9 January 2008
DOI 10.1002/cne.21663
Published online in Wiley InterScience (www.interscience.wiley.com).

ARs of α_2 and β types have been identified in the nervous system and skin of some teleost species (Holmgren and Nilsson, 1982; Svensson et al., 1993; Katayama et al., 1999; Zikopoulos and Dermon, 2005), including zebrafish (Ruuskanen et al., 2004, 2005a,b). The α_{2A}-ARs are located both postsynaptically and presynaptically, the latter limiting the release of NA and other neurotransmitters, such as serotonin and glutamate. This subtype is involved in many physiological processes in birds and mammals, including autonomic functions, sleep-wake cycle, locomotion, reproductive behavior, response to stress, development, visualization, learning, and cognitive processes (Ci-

Abbreviations

A	anterior thalamic nucleus
ALLN	anterior lateral line tract
AR	adrenoceptor
ATN	anterior tuberal nucleus
CC	cerebellar crest
CCe	corpus cerebelli
CCe gr	granular layer of CCe
CCe mol	molecular layer of CCe
Chor	horizontal commissure
CIL	central nucleus of the inferior lobe
CO	optic chiasm
CON	caudal octavolateralis nucleus
CP	central posterior thalamic nucleus
CPN	central pretectal nucleus
Cpost	posterior commissure
Ctec	tectal commissure
D	dorsal telencephalic area
DAO	dorsal accessory optic nucleus
Dc	central zone of dorsal telencephalic area
Dd	dorsal zone of dorsal telencephalic area
DIL	diffuse nucleus of the inferior lobe
DiV	diencephalic ventricle
Dl	lateral zone of dorsal telencephalic area
Dm	medial zone of dorsal telencephalic area
DOT	dorsomedial optic tract
Dp	posterior zone of dorsal telencephalic area
DP	dorsal posterior thalamic nucleus
DTN	dorsal tegmental nucleus
DV	descending trigeminal root
ECL	external cellular layer of olfactory bulb
EG	granular eminence
ENd	entopeduncular nucleus, dorsal part
ENv	entopeduncular nucleus, ventral part
EW	Edinger-Westphal nucleus
FR	habenulointerpeduncular tract
GC	central gray
GL	glomerular layer of olfactory bulb
Had	dorsal habenular nucleus
Hav	ventral habenular nucleus
Hc	caudal zone of periventricular hypothalamus
Hd	dorsal zone of periventricular hypothalamus
Hv	ventral zone of periventricular hypothalamus
IAF	inner arcuate fibers
ICL	internal cellular layer of olfactory bulb
IN	intermediate nucleus
IO	inferior olive
IR	inferior raphe
IRF	inferior reticular formation
LC	locus coeruleus
LCa	caudal lobe of cerebellum
LCa gr	granular layer of LCa
LCa mol	molecular layer of LCa
LFB	lateral forebrain bundle
LH	lateral hypothalamic nucleus
LLF	lateral longitudinal fascicle
LOT	lateral olfactory tract
LR	lateral recess of diencephalic ventricle
LX	vagal lobe
LVII	facial lobe
MA	Mauthner axon
MAO	monoamine oxidase
MaON	magnocellular octaval nucleus
MFB	medial forebrain bundle
MLF	medial longitudinal fascicle
MNV	mesencephalic nucleus of the trigeminal nerve
MON	medial octavolateralis nucleus
MOT	medial olfactory tract
NA	noradrenaline
NI	isthmic nucleus
NIn	interpeduncular nucleus
NLV	nucleus lateralis valvulae
NMLF	nucleus of the medial longitudinal fascicle
NT	nucleus taeniae
NIII	oculomotor nucleus
NIV	trochlear nucleus
NXm	vagal motor nucleus
OT	optic tract
P	posterior thalamic nucleus
PCN	paracommissural nucleus
PGl	lateral preglomerular nucleus
PGm	medial preglomeroular nucleus
PGZ	periventricular gray zone of optic tectum
PL	perilemniscal nucleus
PM	magnocellular preoptic nucleus
PPa	parvocellular preoptic nucleus, anterior part
PPd	periventricular pretectal nucleus, dorsal part
PPp	parvocellular preoptic nucleus, posterior part
PPv	periventricular pretectal nucleus, ventral part
PSm	magnocellular superficial pretectal nucleus
PSp	parvocellular superficial pretectal nucleus
PTN	posterior tuberal nucleus
Rm	medial raphe nucleus
RV	rhombencephalic ventricle
SAC	stratum album centrale
SC	suprachiasmatic nucleus
SFGS	stratum fibrosum et griseum superficiale
SGC	stratum griseum centrale
SGN	secondary gustatory nucleus
SGT	secondary gustatory tract
SM	stratum marginale
SO	stratum opticum (in TeO)
SO	secondary octaval population
SRF	superior reticular formation
T	tangential nucleus
TelV	telencephalic ventricle
TeO	optic tectum
TH	tyrosine hydroxylase
TL	longitudinal torus
TLa	lateral torus
TMC	mesencephalocerebellar tract
TPM	pretectomammilary tract
TPp	periventricular nucleus of posterior tuberculum
TS	semicircular torus
TTB	tectobulbar tract
TTBc	crossed tectobulbar tract
TTBr	uncrossed tectobulbar tract
TVS	vestibulospinal tracts
Va	valvula cerebelli
Val	lateral division of valvula cerebelli
Vam	medial division of valvula cerebelli
Vc	central nucleus of ventral telencephalic area
Vd	dorsal nucleus of ventral telencephalic area
Vl	lateral nucleus of ventral telencephalic area
VL	ventrolateral thalamic nucleus
VM	ventromedial thalamic nucleus
VOT	ventrolateral optic tract
Vp	postcommissural nucleus of ventral telencephalic area
Vs	supracommissural nucleus of ventral telencephalic area
Vv	ventral nucleus of ventral telencephalic area
V	trigeminal nerve
VII	facial nerve
VIII	octaval nerve
X	vagal nerve

riello et al., 1989; Goodman et al., 1996; Hein and Kobilka, 1997; Revilla et al., 1998; Stamatakis et al., 1998; Kable et al., 2000; Riters et al., 2002). In zebrafish, the functional role of the α_2-ARs is not known, but it has been suggested that the A subtype is functional in vivo, insofar as the α_2 agonist dexmedetomidine and the antagonist atipamezole induce sedation and skin color changes (Ruuskanen et al., 2005b). The α_{2A}-AR distribution has been previously studied in many vertebrates, including mammalian (U'prichard et al., 1977; Morris et al., 1981; Leibowitz et al., 1982; Rainbow et al., 1984; Probst et al., 1984), avian (Dermon and Kouvelas, 1988, 1989; Ball et al., 1989; Fernandez-Lopez et al., 1990, 1997), amphibian (Bachman et al., 1998), and teleost fish (Ruuskanen et al., 2005a; Zikopoulos and Dermon, 2005) brains.

The zebrafish, a new model organism for neurosciences, not having undergone major adaptive modifications within the teleost lineage, is suggested to be a useful reference for comparative studies (Rupp et al., 1996). The catecholaminergic system of the zebrafish brain has been previously characterized (Ma, 1994a,b, 1997; Kaslin and Panula, 2001; Rink and Wullimann, 2001), and cerebral neurochemical studies have established the LC as the major noradrenergic projection center of the zebrafish (Ma, 1994a,b; Kaslin and Panula, 2001) and most teleosts (Parent, 1983; Ekström et al., 1986). The LC projection pattern (Ekström et al., 1986; Ma, 1994b) and recently the localization of the monoamine oxidase (MAO), the NA metabolic pathway enzyme (Anichtchik et al., 2006) have been reported for the zebrafish brain. Furthermore, α_2-ARs have been identified in zebrafish, by cloning and mapping of five distinct receptor genes (Ruuskanen et al., 2004), each coding for a functional receptor coupled to G-mediated second messenger signaling system, similar to the mammalian α_2-ARs (Ruuskanen et al., 2005a). Specifically, three of the zebrafish *adra2* genes code for the orthologues of the human α_{2A}-AR, α_{2B}-AR, and α_{2C}-AR, whereas the two genes code for α_{2Da}- and α_{2Db}-AR subtypes, representing a duplicated fourth α_2-AR subtype (Ruuskanen et al., 2004, 2005a). Although it is difficult to establish homologies among vertebrate functional neural systems, the distribution pattern of α_2-AR subtypes in all brain regions would provide a better understanding of their possible role in the zebrafish brain and illuminate comparative aspects of noradrenergic systems in vertebrates. The present study aimed to map the α_{2A}-ARs, the most widely distributed α_2-AR subtype in the vertebrate brain, and to question their neuronal or glial localization, adding important knowledge on the neuroanatomical organization of the noradrenergic transmission in the adult zebrafish brain.

MATERIALS AND METHODS

Animals

Adult (7 months to 1 year old) wild-type zebrafish (Cyprinidae, *Danio rerio*) of both sexes were used in this study. All fish were obtained from aquaculture laboratory (Biology Department, University of Crete) and maintained at 28.5°C on a 14-hour:10-hour light/dark cycle, according to Westerfield (1995). All experimental procedures were in accordance with the European Communities council directive (86/609/EEC) for the care and use of laboratory animals.

Tissue preparation

All fish (n = 21) were anesthetized with a lethal dose of 0.1% tricaine methane sulfonate (MS-222; Sigma, Deisenhofen, Germany) and intracardially perfused with saline (0.9% NaCl), followed by 4% paraformaldehyde (PFA) freshly depolymerized in phosphate-buffered saline (PBS; 0.01 M, pH 7.4). The brains were removed carefully, postfixed in 4% PFA in PBS for 2 hours at 4°C, cryoprotected overnight in 20% sucrose in phosphate buffer (PB; 0.1 M, pH 7.4) at 4°C, rapidly frozen in dry-ice-cooled isopentane (2-methylbutane; Sigma) at approximately –35°C, and stored at –80°C until use. Before cutting in a cryostat (CM1500; Leica, Wetzlar, Germany) at a transverse coronal plane (section thickness 20 μm), the brains were embedded in tissue freezing medium (Jung; Leica). All sections were collected serially on gelatin-coated slides, air-dried for 1 hour, and processed for immunohistochemistry.

Antibody specificity

Goat anti-α_{2A} adrenoceptor polyclonal antibody. A α_{2A}-AR subtype antibody was obtained from Santa Cruz Biotechnology (Santa Cruz, CA; catalog No. sc 1478; lot No. C0404). The polyclonal antibody was raised against synthetic peptide (DFRRAFKKILCRGDRKRIV) corresponding to amino acids 431–450 of the carboxy-terminus of the α_{2A}-AR of human origin (Swiss Prot protein accession No. P08913; lot No. C0404; Nasser et al., 2006). Further details for the antibody can be found at the manufacturer's website (http://www.scbt.com). The specificity of this antibody in teleost brain has been documented by Western blot of brain protein extracts in the red porgy (*Pagrus pagrus*; Zikopoulos and Dermon, 2005) and by preabsorption with its respective antigen for immunocytochemistry on brain slices (Zikopoulos and Dermon, 2005; Nasser et al., 2006).

To test the specificity of the primary α_{2A} antibody in the teleost tissue, several control experiments were performed in adjacent sections, including 1) omission of the primary antibodies, 2) application of secondary antisera mismatched for species, and 3) application of preincubated primary goat anti-α_{2A}AR (Santa Cruz Biotechnology; sc 1478; lot No. C0404; dilution 1:50) with excess of the specific peptide used to raise the α_{2A}-AR antibody (Santa Cruz Biotechnology; sc 1478P for α_{2A}AR; lot No. I0704; dilution 1:5). All control experiments resulted in no immunocytochemical labeling in any brain area, and staining of the α_{2A}-AR was completely abolished when preincubated with the blocking peptide (10 μg/250 μl).

Moreover, the staining pattern in zebrafish brain obtained from this antibody is in close relation to the distribution pattern previously reported based on in vitro receptor autoradiography in a marine teleost brain (pagrus; Zikopoulos and Dermon, 2005) and the pattern described using in situ hubridization with mRNA probes to zebrafish *adra2* gene and in vitro receptor autoradiography in zebrafish brain (Ruuskanen et al., 2005b).

Mouse anti-HuC/D monoclonal antibody. The mouse IgG_{2b}, anti-HuC/HuD neuronal protein (human) was obtained from Molecular Probes (Eugene, OR; catalog No. A-21271; lot No. 71C1-1). This antibody recognizes the Elav family members HuC, HuD (RNA-binding proteins), and Hel-N1, which are all neuronal proteins. The presence of Hu proteins serves as a marker for newly committed postmitotic neuronal cells of the CNS as well as for mature

neurons (Marusich et al., 1994; Barami et al., 1995). This antibody has been shown to label specifically neuronal cells in zebrafish, chick, canaries, and humans and is likely to label neuronal cells in most vertebrate species. In addition, the staining pattern observed in the present study using this antibody is identical to that previously shown in the zebrafish nervous system (Byrd and Brunjes 2001; Mueller and Wullimann, 2002; Grandel et al., 2006).

Mouse antiglial fibrillary acidic protein monoclonal antibody. The mouse antiglial fibrillary acidic protein (GFAP; IgG_1 isotype) was obtained from Sigma (lot No. 033K4869; catalog No. G3893). The antibody stains astrocytes and radial glia and some types of ependyma cells in most vertebrates (Levitt and Rakic, 1980; Bodega et al., 1990, 1993, 1994; Eng et al., 2000). Previous studies have establish the specificity of this antibody for labeling teleost glial elements (Nielsen and Jorgensen 2003; Alumni et al., 2005; Zupanc et al., 2005). The staining pattern found in the present study is in agreement with the previously established glial morphology in teleosts.

Rabbit anti-DβH polyclonal antibody. Immunohistochemical detection of the catecholamine synthesis enzymes tyrosine hydroxylase (TH) and DβH (partially cloned in zebrafish; Guo et al., 1999) in zebrafish brain was carried out according to previously published protocols (Kaslin and Panula, 2001; Kaslin et al., 2004). Rabbit anti-DβH (Chemicon, Temecula, CA; lot Nos. 23040925 and 21100238; catalog No. AB1538) raised against synthetic peptide CSAPRESPLPYHIPLDPEG-amide, cloned from human (DβH) cDNA, was used. By immunoblot, the antibody specifically reacts with a single (or double) band(s) of M.W. >70,000–75,000 in samples of sodium dodecyl sulfate (SDS)-solubilized, dithiothreitol (DTT)-reduced human adrenal medulla subjected to SDS-PAGE. The observed staining pattern of DβH was identical to that described previously in adult zebrafish brain (Kaslin and Panula, 2001)

Mouse anti-TH monoclonal antibody. The monoclonal ($IgG_{1\kappa}$) mouse anti-TH was obtained from Chemicon (catalog No. MAB318; lot No. 21121038). The antibody recognizes an epitope outside the regulatory N-terminus of TH and by Western blot recognizes a protein of approximately 59–63 kDa. Studies in teleosts have established the specificity of this antibody in the teleost brain (Ma, 2003), and the present data are in agreement with the previously described pattern in adult zebrafish brain (Kaslin and Panula, 2001).

Mouse antiparvalbumin monoclonal antibody. A mouse monoclonal (IgG_1), antiparvalbumin (PV) antibody was obtained from SWant (Bellinzona, Switzerland; lot. No. 10-11(F); catalog No. 235). The antibody was completely characterized (Celio et al., 1988) and specifically stains the ^{45}Ca-binding spot of PV (MW 12,000 and IEF 4.9) in a two-dimensional immunoblot. The staining pattern observed in adult zebrafish brain in the present study is comparable to the previously established distribution pattern in mammalian (Celio, 1990; Bu et al., 2003), avian (Wild et al., 2005), and teleostean (Alonso et al., 1992; Porteros et al., 1998; Crespo et al., 1999) brain.

Mouse antibromodeoxyuridine monoclonal antibody. A mouse monoclonal ($IgG_{1\kappa}$) antibromodeoxyuridine (BrdU) antibody was obtained from Becton Dickinson (Franklin Lakes, NJ; clone B44; lot No. 76338; catalog No. 347580). BrdU is a uridine derivative that can be incorporated into DNA in place of thymidine. Anti-BrdU identifies BrdU (but not thymidine) in single-stranded DNA. The monoclonal antibody against BrdU and has been used previously in zebrafish (Zupanc et al., 2005; Ampatzis and Dermon, 2007) and other teleost species (Zikopoulos et al., 2000) brain, with similar distribution patterns of adult proliferation zones.

Mapping of α_{2A}-AR immunoreactivity

Single-labeling experiments (n = 10) were performed to determine the detailed distribution pattern of α_{2A}-ARs. For this, serial sections were washed for 10 minutes with 3% H_2O_2 in PBS for 10 minutes at room temperature (RT), to inhibit endogenous peroxidase activity, followed by three washes for 5 minutes each in PBS. Nonspecific protein binding sites were blocked with 0.15% normal horse serum (NHS) with 5% bovine serum albumin (BSA) and 0.5% Triton X-100 in PBS for 30 minutes at RT. They were then incubated for 20–30 hours at 10°C in a moist chamber with goat anti-α_{2A}-AR (diluted 1:50–1:150 in PBS with 0.5% Triton X-100). The sections were rinsed in PBS three times for 5 minutes each and incubated with a biotynilated anti-goat antibody (Vector, Peterborough, United Kingdom; diluted 1:200 in PBS) for 3 hours at RT. Then, the sections were washed three times in PBS with 0.5% Triton X-100 and then were incubated in Vectastein Elite ABC reagent (Vector; dilution 1:100A and 1:100B) in PBS with 0.5% Triton X-100n for 1 hour in the dark at RT and washed with PBS. The immunoreaction was revealed with 3,3′-diaminobenzidine (DAB; Vector). Methyl green was used to counterstain (Sigma; 1% methyl green in ddH_2O) and facilitate the identification of brain regions. The sections were then dehydrated and cleared with xylene and coverslipped with Entellan (Merck, Darmstadt, Germany).

Double labeling of α_{2A}-AR immunoreactivity with neuronal/glial markers

To identify the phenotype of cells expressing α_2-AR subtypes, additional experiments were performed for double-labeling studies (n = 9) using the primary antibodies described in Table 1. Brain sections were incubated with a mixture of primary antibodies of polyclonal anti-α_{2A}-AR (diluted 1:50 in PBS with 0.5% Triton X-100), with monoclonal anti-HuC/D (diluted 1:100), or with monoclonal anti-TH antibody (diluted 1:1000), with monoclonal antibody against GFAP (diluted 1:100), with polyclonal anti-DβH (diluted 1:250), with monoclonal anti-PV (diluted 1:2,500–1:5,000), or with monoclonal anti-BrdU (diluted 1:100) for 20–48 hours at 10°C. A mixture of secondary antibodies anti-goat Alexa fluor 488 or 568p; anti-rabbit Alexa fluor 350, 488, or 568; and anti-mouse Alexa fluor 350, 488, or 568 (Molecular Probes, Leiden, The Netherlands; diluted 1:500 in 0.5% Triton X-100 in PBS) were used in these experiment. The secondary antibody cocktail was added to the sections for 3 hours at RT in the dark. The sections were thoroughly rinsed in PBS and coverslipped with fluorescent hard medium (Vector; H-1400).

In addition, three adult zebrafish were anesthetized with 0.02% tricaine methanesulfonate (MS 222; Sigma) and injected intraperitoneally with a single dose of a saline-BrdU solution (Sigma; 0.2 mg/g body weight). Fish were allowed to survive for 21 days (long-term survival). To visualize incorporated BrdU, DNA denaturation was performed by incubating the sections in 2 N HCl for 30 minutes at 37°C.

TABLE 1 Primary Antibody Characterization

Antibody	Source	Host species	Epitope	Dilution	Stains	References[1]
α_{2A}-AR (C-19)	Santa Cruz Biotechnology (sc 1478)	Goat	C-terminus (h): amino acids 400-450B	1:50-1:150	Adrenergic receptors (ARs)	5,11,12,14
HuC/D	Molecular Probes (mAb 16A11)	Mouse	RNA-binding proteins of Elav family	1:100	Neuronal proteins (HuC, HuD, Hel-Nl)	4,8,10
TH	Chemicon (MAB318)	Mouse	N-terminus	1:1,000	Dopaminergic, adrenergic neurons and chromaffin tissue	6
DβH	Chemicon (AB1538)	Rabbit	N-terminus	1:250	Noradrenergic and adrenergic neurons, noradrenergic processes	6
GFAP	Sigma, clone G-A-5 (G3893)	Mouse	GFAP (50 kDa)-specific IF protein in astrocytes	1:100	Astrocytes, Bergman glia, and chondrocytes of elastic cartilage	3,7
PV	SWant (235)	Mouse	^{45}Ca-binding spot of parvalbumin	1:2,500-1:5,000	Parvalbumin calcium-binding protein	1,2,13
BrdU	Becton Dickinson, clone B44	Mouse	Incorporated bromodeoxyuridine	1:100	Cell proliferation and activation	9

[1]1) Celio et al., 1988; 2) Crespo et al., 1999; 3) Eng et al., 2000; 4) Grandel et al., 2006; 5) Hou et al., 2002; 6) Kaslin and Panula, 2001; 7) Levitt and Rakic, 1980; 8) Marusich et al., 1994; 9) Miller and Nowakowski, 1988; 10) Mueller and Wullimann, 2002; 11) Modirrousta et al., 2005; 12) Ohshita et al., 2004; 13) Porteros et al., 1998; 14) Zikopoulos and Dermon, 2005.

Western immunoblotting

Western immunoblot experiments were performed for α_{2A}-AR antibody to compare the migration of the immunoreacting proteins in mammalian (rat) and zebrafish brains. Zebrafish (*Danio rerio*; n = 2) and rat (*Rattus norvegicus*; n = 2) brain tissues were homogenized with a Teflon-glass homogenizer in 0.01 M PBS, pH 7.4, containing 1% Triton X-100 (Sigma), 0.5% sodium deoxycholate (Sigma), and 0.05% SDS (Sigma). Iodoacetamide (1 mM; Sigma), 0.4 mM phenylmethylsulfonyl fluoride (PMSF; Sigma), and 1 μM pepstatin A (Sigma) were used as protease inhibitors. The tissue homogenates were incubated in ice for 1 hour and further homogenized by passing through a 22-gauge needle. Remaining cell debris was removed by brief centrifuging at 8,000 rpm for 20 minutes at 4°C. The supernatant was used for protein concentration determination via Lowry assay and subsequently was diluted with loading buffer (2 ml 0.5 M Tris-HCl, 1.6 ml glycerol, 3.0 ml 10% SDS, 0.8 M mercaptoethanol, 0.4 ml 0.05% bromophenol blue) accordingly, then boiled for 5 minutes at 95°C. Twenty micrograms of protein was separated electrophoretically in a 10% SDS-polyacrylamide gel. The separated proteins were transferred to nitrocellulose membrane at 400 mA for 2 hours at 4°C and subsequently stained briefly with Poinceau red to verify protein transfer. After blocking with 5% nonfat dried milk and 1% NHS in PBS-Tween (0.05% Tween-20 in 0.01 M PBS) for 60 minutes, the membranes were incubated with the α_{2A}-AR goat polyclonal antibody (Santa Cruz Biotechnology; diluted 1:200 in PBS-Tween with 2% nonfat dried milk) at 10°C for 24 hours. After three washes in PBS-Tween for 10 minutes each, the membranes were incubated for 2 hours at RT with secondary anti-goat IgG antibodies (Vector ABC Elite kit) diluted 1:2,000 in PBS-Tween, followed by an avidin-biotin-peroxidase solution (Vector ABC Elite kit; diluted 1:1,000A and 1:1,000B in PBS-Tween) for 1 hour in the dark at RT. Bands were visualized by the peroxidase-catalyzed polymerization of 0.05% diaminobenzidine solution (DAB; Vector) in 0.01% H_2O_2 buffer solution (pH 7.5). Rat brain homogenates were used as positive controls, whereas omission of primary antibodies provided the necessary negative controls.

Brain anatomy, microscopy, and photomicrograph processing

The nomenclature used was based on the zebrafish brain atlas of Wullimann et al. (1996). All images were collected using a 3CCD Sony DXC-950P camera adjusted on an optical and fluorescent microscope (Nikon Eclipse E800) connected to a PC (Windows XP) via a Scion CG-7 frame grabber (Scion Corp.). Stacks of optically sliced images were generated in Scion Image Image B4.0.2 (Scion Corp.) and further used for identification of double-labeled cells and for image processing. Figures were prepared with Adobe Photoshop CS2 (Adobe Systems Inc., San Jose, CA), and graphs were prepared in Corel Draw 11 (Corel, Dallas, TX) for Macintosh (MacOS 10.4). All double-labeled images were converted to magenta-green immunofluoresence to make this work more accessible to the 6–10% of male red-green color-blind readers.

RESULTS

Western blot analysis and specificity of α_{2A}-AR antibody

The polyclonal α_{2A}-AR subtype-specific antibody, generated against mammalian adrenoceptor proteins, recognized homologous proteins from zebrafish, protein extracts from rat and zebrafish brains processed by SDS-PAGE and Western blotting. Specifically, the polyclonal α_{2A}-AR antibody detected a protein band migrating at the same apparent molecular weight as the corresponding rat AR proteins (Fig. 1), possibly representing the zebrafish homologues of AR. In addition, previous Western blot experiments showed similar molecular weight of protein bands of rat and teleostean (red porgy) brain, specifically reacting with the same anti-α_{2A}-AR polyclonal antibody (Zikopoulos and Dermon, 2005). Moreover, preabsorption with excess (tenfold) of the specific peptide used to raise the α_{2A}-AR antibody completely abolished the labeling in all brain regions in the presence of the relevant primary and secondary antibodies. Taken together, these data support the specificity of the anti-α_{2A}-AR labeling in the zebrafish brain.

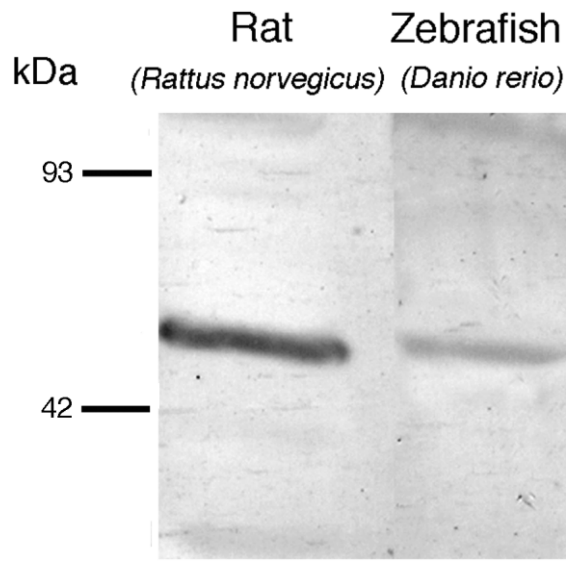

Fig. 1. Western blot analysis of the α_{2A}-ARs, using rat (*Rattus norvegicus*) and zebrafish (*Danio rerio*) brains. Note the stronger expression of α_{2A}-AR proteins in the rat compared with the zebrafish brain, in agreement with the lower levels of adrenoceptors in the zebrafish brain.

Localization of α_{2A}-AR immunoreactivity in adult zebrafish brain

General features. α_{2A}-AR-ir cells and fibers were found characteristically in distinct clusters or scattered in all major brain divisions of the adult zebrafish brain. The labeling pattern showed a medial to lateral and caudal to rostral gradient, with higher densities in the periventricular and caudal planes. Intense labeling of α_{2A} immunoreactivity characterized the surface of the ventricles, related possibly to the ependymal lining, as well as the periventricular areas. In addition, significant α_{2A}-AR labeling was found in association with blood vessels and pial surface. Several cell types and elements were identified to express α_{2A}-ARs. Specifically, adrenoceptor-like immunoreactivity was related to 1) small ($\leq$5 μm) cells with diffuse or with punctate labeling found in most of the periventricular areas of the adult zebrafish brain, 2) medium-sized ($\sim$10 μm) and large ($\geq$20 μm) multipolar cells with thick dendrites in the rhombencephalon, around the fourth ventricle (darkly stained or with punctuate labeling, such as in the LC and in the ganglionic cell layer of the cerebellum, respectively), 3) fibers and varicosities found in the periventricular areas and commissures, and 4) nerves and roots such as the descending trigeminal root (DV). In addition, there was staining in the neuropil, diffuse and more often punctate, without clear somata or fiber-like morphology, in agreement with the staining pattern of mRNA and enzymatic activity of MAO (Anichtchik et al., 2006). Detailed mapping of the expression of the α_{2A}-AR is shown schematically in Figure 2.

Telencephalon. The zebrafish olfactory bulbs and telencephalic hemispheres included a moderate density of α_{2A}-AR-positive cells and fibers, with the ventral telencephalic area including higher densities (Fig. 2A–C). In the olfactory bulbs, α_{2A}-AR immunoreactivity was observed in fibers and blood vessels, and labeling was confined mainly to the glomerular layer (Figs. 2A, 3A), in agreement with the pattern of noradrenergic nerve terminals (Anichtchik et al., 2006). The medial and lateral zones of the dorsal telencephalon (Dm, Dl), along the telencephalic ventricle, exhibited moderate labeling of α_{2A}-AR fibers (Figs. 2B–E, 3B). In the central zone of dorsal telencephalic area (Dc) large thick fibers were observed (Figs. 2B–D, 3D). A low density of α_{2A}-AR-ir fibers and neuropil was found in the dorsal zone and in the posterior zone of dorsal telencephalic area (Dd, Dp; Figs. 2C–E, 3C). However, in the lateral, ventral, and dorsal nucleus of the ventral telencephalic area (Vl, Vv, Vd) and in the postcommissural nucleus of the ventral telencephalic area (Vp), moderate to high levels of α_{2A}-AR-immunopositive fibers were observed (Figs. 2A–D, 3E). Many immunoreactive bundles of fibers were observed in the lateral olfactory tract (LOT) neighboring the lateral nucleus of the ventral telencephalic area (Vl; Figs. 2B, 3G).

In contrast to neuropil and fiber labeling, few α_{2A} AR-positive cells were found in the medial zone of dorsal telencephalic area (Dm; Fig. 3B), the central and posterior nucleus of dorsal telencephalic area (Dc, Dp; Fig. 3C,D). In the ventral telencephalon, high numbers of α_{2A}-AR-immunopositive cell bodies and fibers were found in the ventral nucleus of the ventral telencephalic area (Vv; Fig. 2B,C), but only few immunopositive cells were detected in the dorsal nucleus of the ventral telencephalon (Vd; Fig. 3E), in the supracommisural nucleus of the ventral telencephalic area (Vs), or in the postcommissural nucleus of the ventral telencephalic area (Vp). The described pattern of α_{2A}-AR localization is in general agreement with the relative density of zebrafish noradrenergic terminals (Ma, 1994b) and MOA activity (Anichtchik et al., 2006). No α_{2A}-ARs labeling was found in medial (MFB) and lateral (LFB) forebrain bundle, although the former has been reported to be closely associated withj the longitudinal catecholamine bundle (Ma, 2004b).

Preoptic region. In the preoptic area, a moderate density of adult zebrafish α_{2A}-immunopositive cells and fibers was observed in the anterior parvocellular preoptic nucleus (PPa; Figs. 2D, 3F), Intense, diffuse labeling characterized posterior parvocellular preoptic nucleus (PPp) as well as a great portion of immunostained fibers and α_{2A}-AR-immunopositive cells (Figs. 2E,F, 4A). In contrast to strong MAO activity (Anichtchik et al., 2006), the suprachiasmatic nucleus (SC) included stained fibers only in its dorsolateral compartment (Fig. 2E). In addition, the magnocellular preoptic nucleus (PM) was characterized by a high density of α_{2A}-AR-labeled cells but few fibers (Figs. 2E, 4B).

Diencephalon. Epithalamus, dorsal thalamus, ventral thalamus, posterior tuberculum, hypothalamus, and synencephalon are included in the diencephalon according to the zebrafish topological atlas (Wullimann et al., 1996). In the epithalamic, thalamic, and hypothalamic regions, dense labeling of α_{2A}AR-immunostained elements was observed in all periventricular nuclei (Fig. 2). In addition, we detected a significantly high number of labeled blood vessels. The epiphysis and lateral habenular nuclei exhibited strong α_{2A}-AR labeling, in agreement with the thick noradrenergic axons described in the habenular complex (Anichtchik et al., 2006).

In the superficial pretectum, the magnocellular nucleus (PSm) and the parvocellular nucleus (PSp) were charac-

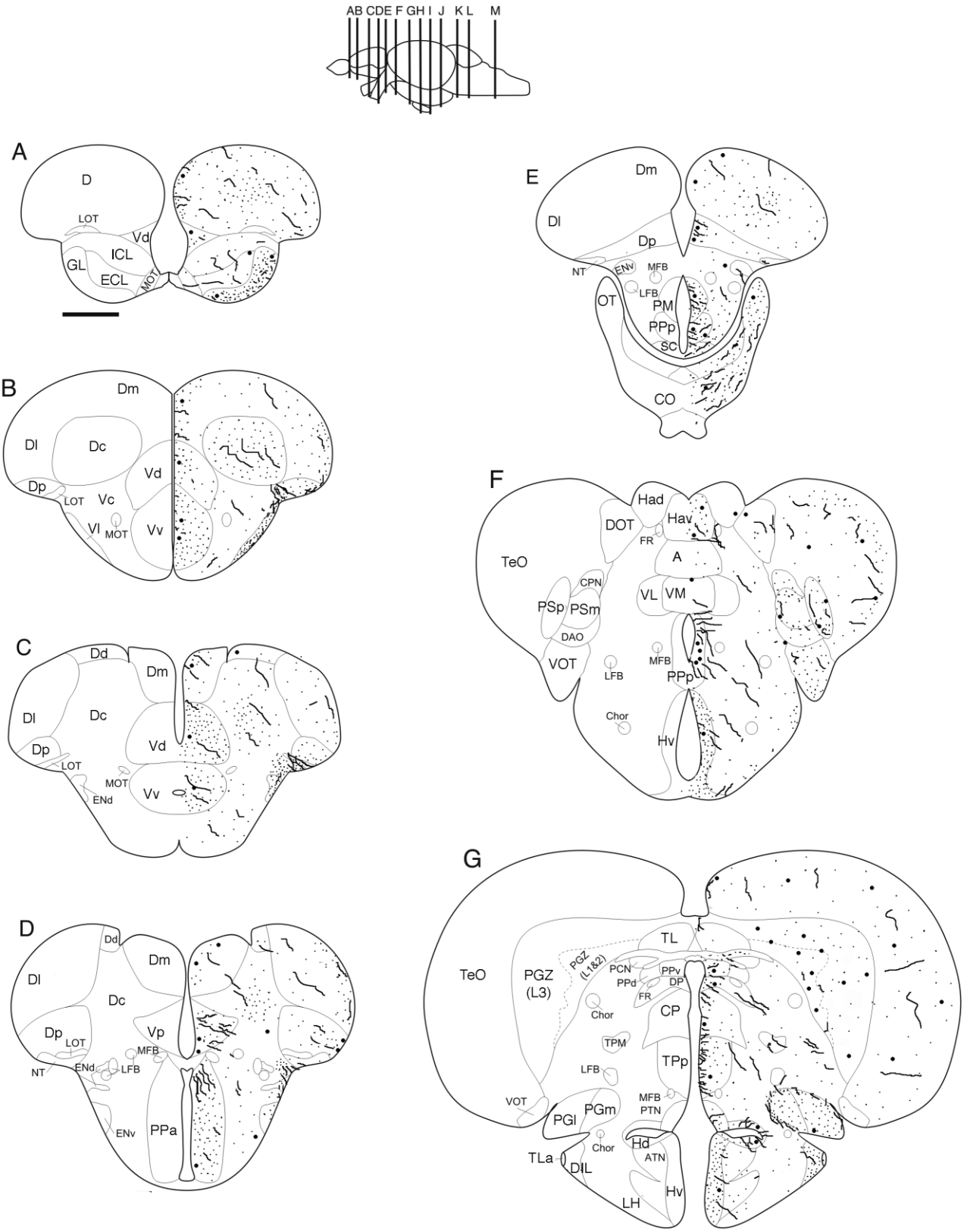

Fig. 2. Schematic drawings of transverse sections of the adult zebrafish brain showing, at right, the distribution of α_{2A}-AR-immunoreactive cells (solid circles), fibers (curved lines), and varicose fibers (dotted areas) and, at left, the brain nuclei and regions according to Wullimann et al. (1996). The anteroposterior level (**A-M**) of the sections is presented in the lateral view of the adult zebrafish brain, at the top of the figure. For abbreviations see list. Scale bars = 200 μm.

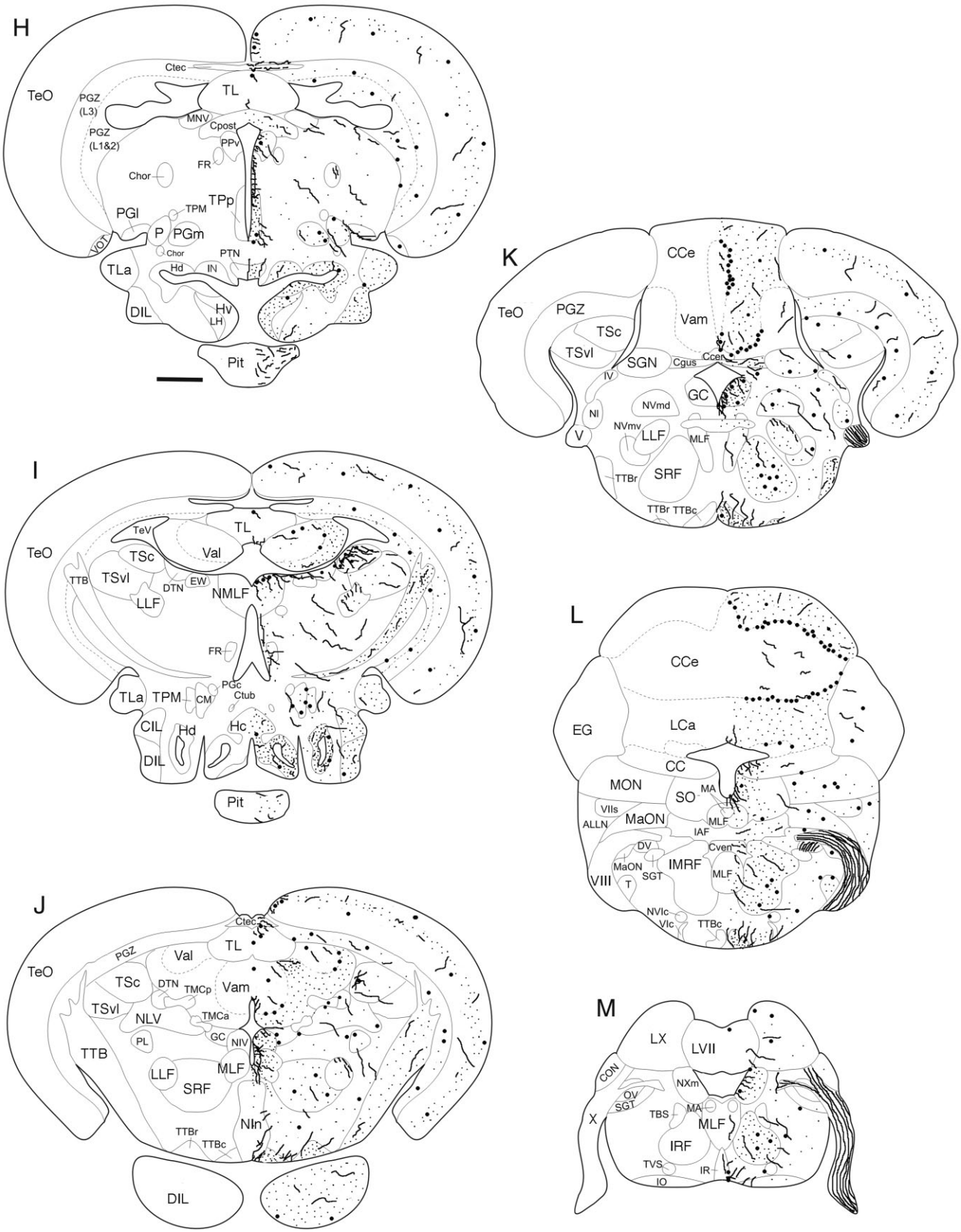

Figure 2 (Continued)

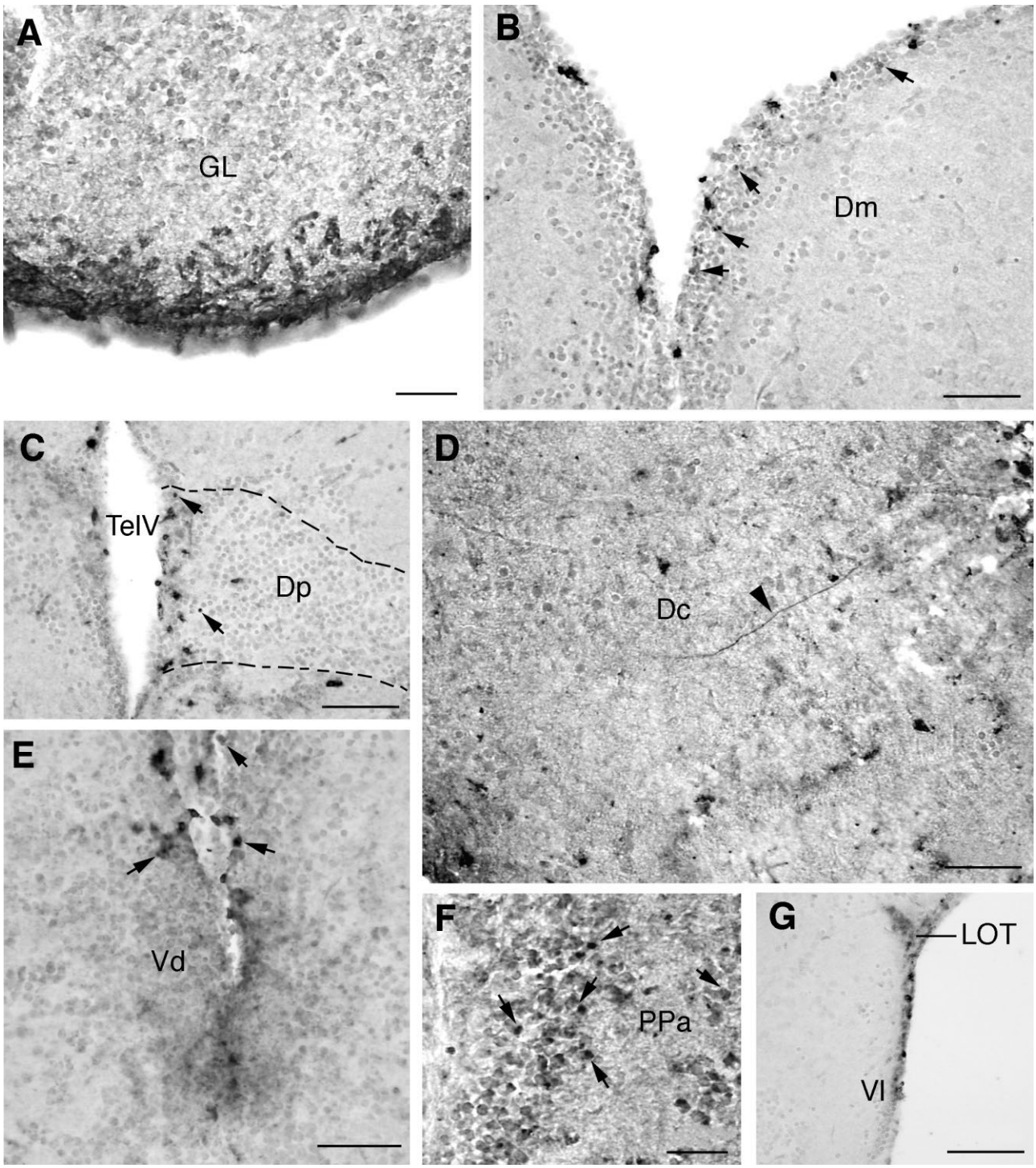

Fig. 3. Photomicrographs of sections of the forebrain showing selected regions immunoreactive for α_{2A}-AR. **A:** α_{2A}-AR immunoreactivity in the glomerular layer of the olfactory bulb. **B:** α_{2A}-AR-immunopositive cells (arrows) and blood vessels in the medial zone of the dorsal telencephalic area. **C:** Arrows indicate small α_{2A}-AR-ir cell profiles that are located in the posterior zone of the dorsal telencephalic area. **D:** Detail of the central zone of the dorsal telencephalic area showing a large thick fiber (arrowhead). **E:** α_{2A}-AR-immunopositive cells (arrows) and blood vessels and innervation of the dorsal nucleus of the ventral telencephalic area. **F:** α_{2A}-AR-positive cells in the preoptic nucleus PPa (arrows). **G:** Immunostained cells and fibers in the Vl and LOT of the adult zebrafish brain. For abbreviations see list. Scale bars = 0.02 mm in A,F; 0.04 mm in B–E,G.

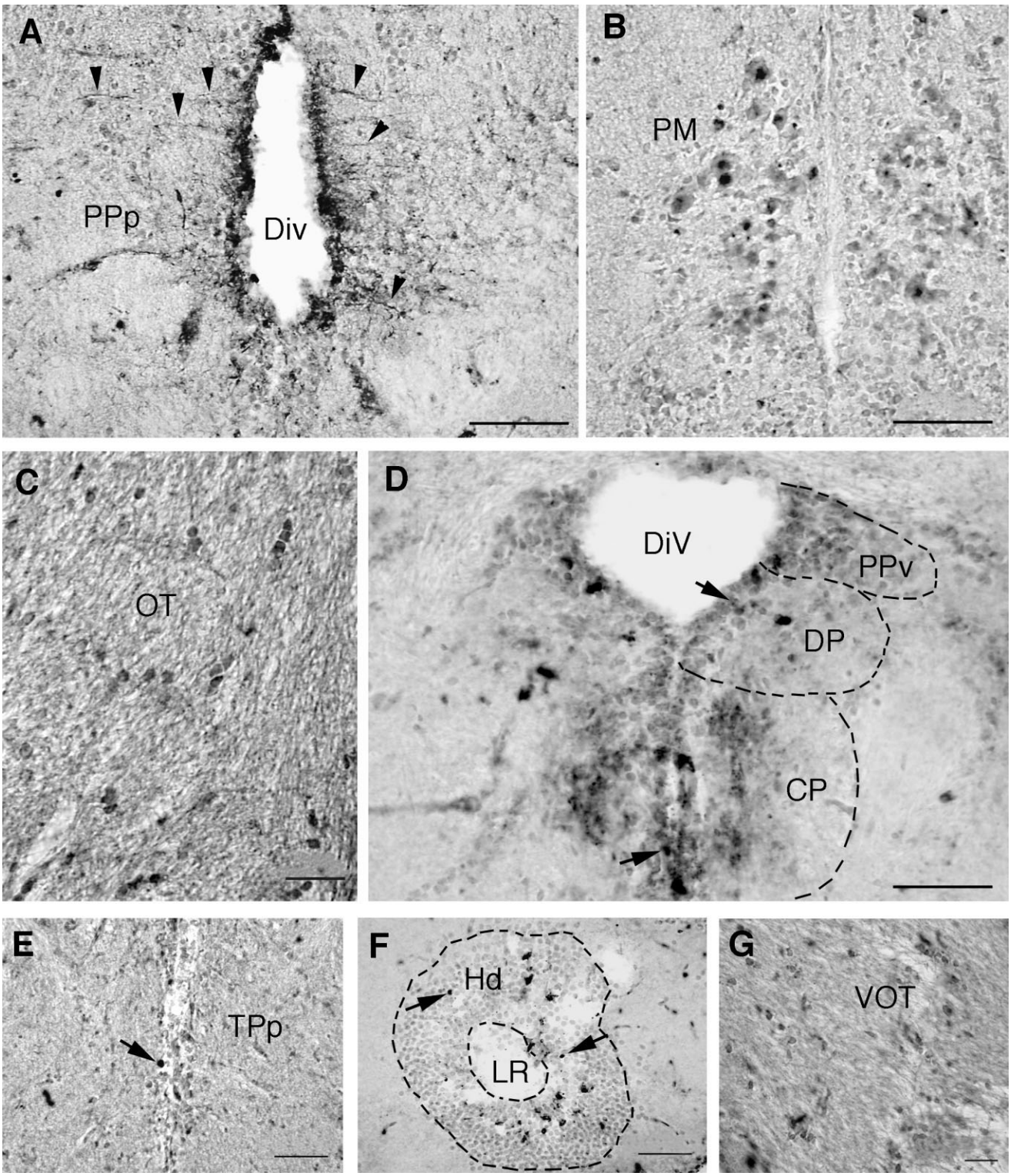

Fig. 4. Photomicrographs of selected sections showing the distribution of α_{2A}-AR-immunoreactive areas in the adult zebrafish diencephalon. **A:** Immunopositive large fibers (arrowheads) with mediolateral orientation in the preoptic nucleus PPp. **B:** α_{2A}-AR immunostaining in the magnocellular preoptic nucleus. **C:** Details of α_{2A}-AR-ir cells and fibers in the optic tract. **D:** Showing details of α_{2A}-AR cells (arrows) and fibers in the periventricular nuclei around the diencephalic ventricle. **E:** Immunopositive cell (arrow) in the periventricular nucleus of the posterior tuberculum. **F:** Cells (arrows) and blood vessels surrounding the dorsal zone of periventricular hypothalamus. **G:** Section showing the α_{2A}-AR ir cell and fiber population in the VOT. For abbreviations see list. Scale bars = 0.05 mm in A,B,D–F; 0.02 mm in C,G.

terized by a dense plexus of α_{2A}-AR-ir fibers, with few scattered cells outlining the borders of the nuclei (Fig. 2F). In the hypothalamus, high numbers of α_{2A}-AR-ir small cells, fibers, and blood vessels were found, particularly in the dorsal, ventral, and caudal zone of periventricular hypothalamus (Hd, Hv, Hc; Figs. 2F–I, 4F). In these nuclei, the characteristic high density of α_{2A}-AR-ir varicosities formed a plexus of fibers. The nuclei of posterior tuberculum were found to have immunostained fibers, cells, or both. For the periventricular nucleus of the posterior tuberculum (TPp), we detected blood vessels and few cells, but significant densities of α_{2A}-AR-ir fibers having a mediolateral orientation, perpendicular to the ventricle (Figs. 2G,H, 4E). In the PGm and PGl (medial and lateral pregromerular nuclei), α_{2A}-AR-ir fibers and cells were also observed (Fig. 2G). In contrast, the corpus mamillare (CM) included moderate numbers of α_{2A}-AR-ir cells but no fibers.

The zebrafish synencephalon is formed by the nucleus of the medial longitudinal fascicle (NMLF), the ventral and dorsal part of periventricular pretectum (PPv, PPd), the paracommissural nucleus (PCN), and the subcommisural organ (SCO). Cells and strongly stained fibers positive for α_{2A}-AR-ir were restricted to the periventricular areas, such as the PPv (Figs. 2G,H, 4D) and the NMLF (Fig. 2I).

The tractus pretectomamillaris (TPM) exhibited very few α_{2A}-AR-immunopositive varicosities forming thin fibers (Fig. 2H). Moderate α_{2A}-AR immunoreactivity was detected in small cells of the subcommissural organ, the periventricular zone of central posterior thalamic nucleus (CP; Figs. 2G, 4D) and posterior tuberal nucleus (PTN). The diffuse nucleus of the inferior lobe (DIL) exhibited low, diffuse immunoreactivity (Fig. 2H–J), although it was shown to exhibit MAO mRNA signal in a sparse population of small cells (Anichtchik et al., 2006).

Mesencephalon. The mesencephalon of zebrafish brain is divided into three different regions: the optic tectum (TeO), the torus semicircularis (TS), and the tegmentum. We found α_{2A}-AR immunoreactivity in all three regions. Immunostained α_{2A}-AR fibers and cells were detected in all layers of the optic tectum (Figs. 2F–K, 5A). Labeled cells were located mainly in the mediodorsal part of the tectum (Fig. 5B). Stratum marginale, stratum griseum superficiale, exhibited moderate α_{2A}-AR labeling in small cells arranged in layers and in fibers crossing layers, oriented radially and perpendicularly. Optic tract (OT) and ventral optic tract (VOT) included a high density of small labeled cells, in addition to the labeled fibers (Figs. 2E–H, 4C,G). The pia mater overlying the optic tectum exhibited strong α_{2A}-AR immunoreactivity in fibers and blood vessels. A great number of stained blood vessels with α_{2A}-AR were also found in the periventricular gray zone of optic tectum (PGZ) as well as in the layers of the TeO. In addition, immunostained round small cells, forming a reticular network, were observed in PGZ (Figs. 2G–K, 5A). The torus longitudinalis (TL) was the only mesencephalic area with rare immunopositive α_{2A}-AR cells or fibers (Fig. 2G–J). In contrast, the TS included high densities of immunoreactive fibers, mainly in its dorsoventricular part (Fig. 2I,J).

The tegmentum included many labeled motor structures, such as the oculomotor (NIII) nucleus, the parasympathetic Edinger-Westphal nucleus (EW), and the nucleus ruber (NR). All of those nuclei included densely laleled large α_{2A}-AR-ir cells and fibers (Fig. 2I–K; 5D). The oculomotor nucleus (NIII) showed a characteristic pattern of high density of stained fibers originating near the tectal ventricle (TeV), with dorsoventral orientation.

Rhombencephalon and cerebellum. For the rhombencephalon (Mueller et al 2004) of adult zebrafish brain, we observed the highest density of immunopositive structures for α_{2A}-AR antibody. Specifically, α_{2A}-AR labeling was localized in large strongly stained cells of the LC (Fig. 5G) and medium-sized cells of the area located medially to the medial longitudinal fascicle (MLF), defined as medial raphe nuclei (Rm) by Kaslin and Panula (2001). In addition, in the trochlear (NIV) nucleus, large cell somata and fibers were densely labeled, similarly to the oculomotor nucleus. Weak labeling was detected in nucleus interpeduncularis (NIn), with strong labeling of fibers and blood vessels in its ventral part (Fig. 2J).

The somata and the proximal dendrites of the neurons in the LC, three to five large neurons dorsal to the superior reticular formation (SRF) were strongly stained for α_{2A}AR, with no neuropil staining. In addition, the griseum centrale (GC), near the rhombencephalic ventricle, contained strong α_{2A}-stained bundles of fibers but few medium-sized cells and several blood vessels (GC; Figs. 2J,K, 5E). The SRF and the intermediate reticular formation (IMRF) included characteristic large α_{2A}-AR-ir cells and fibers (Fig. 2J,K). The inferior reticular formation (IRF) included also small cells in addition to the strongly labeled large cells (Figs. 2M, 5I). The magnocellular octaval nucleus (MaON), located between the tangential nucleus (T) and the sensory root of the facial nerve (VIIs), contained a high number of α_{2A}-AR-ir large cells and fibers (Figs. 2L, 5H).

In the medulla oblongata, all the nerves and nerve roots were positive for α_{2A}-ARs. Specifically, the descending trigeminal root (DV; Figs. 2L, 5F), although it was reported to be devoid of MAO activity (Anichtchik et al., 2006), exhibited a high density of strongly labeled fibers. The tectobulbar tract (TTB), the crossed (TTBc) and uncrossed (TTBr) tectobulbar tract, included a high number of α_{2A}-AR-positive blood vessels along with fibers with characteristic varicosities (Figs. 2I,J, 5C). The dorsal vagal lobes showed a low, punctuate α_{2A}-AR signal in small cells and neuropil. The medial (MLF) and lateral longitudinal fascicles (LLF), lobus facialis, and tractus bulbospinalis included α_{2A}-AR imunoreactivity in fibers (Fig. 2I–M).

In the adult zebrafish cerebellum, α_{2A}-AR-ir was present in all subdivisions (valvula and corpus cerebellum, caudal lobe, eminentia granularis). The laminar pattern of the α_2-AR immunoreactivity was characteristic, with the majority of the cell somata of the ganglionic cell layer (including Purkinje cells and eurydendroid cells) exhibiting strong punctate α_{2A}-AR labeling (Figs. 2I–L, 6A–C). In addition, some small round cells and fibers were observed to be α_{2A}-AR ir in the molecular layers of all cerebellar subdivisions (Figs. 2I–L, 6A). Immunopositive fibers were also found in the granular cell layer (Fig. 2I–L).

Neuronal and glial localization of α_{2A}-ARs

To determine the type of cells (neuronal or glial) expressing α_{2A}-AR, we performed double-immunofluoresence experiments with glial (GFAP) and neuronal (HuC/D, PV) markers. In addition, we questioned whether newborn cells expressed α_{2A}-AR, because high levels of α_{2A}-AR-positive cells were associated with the adult zebrafish proliferation

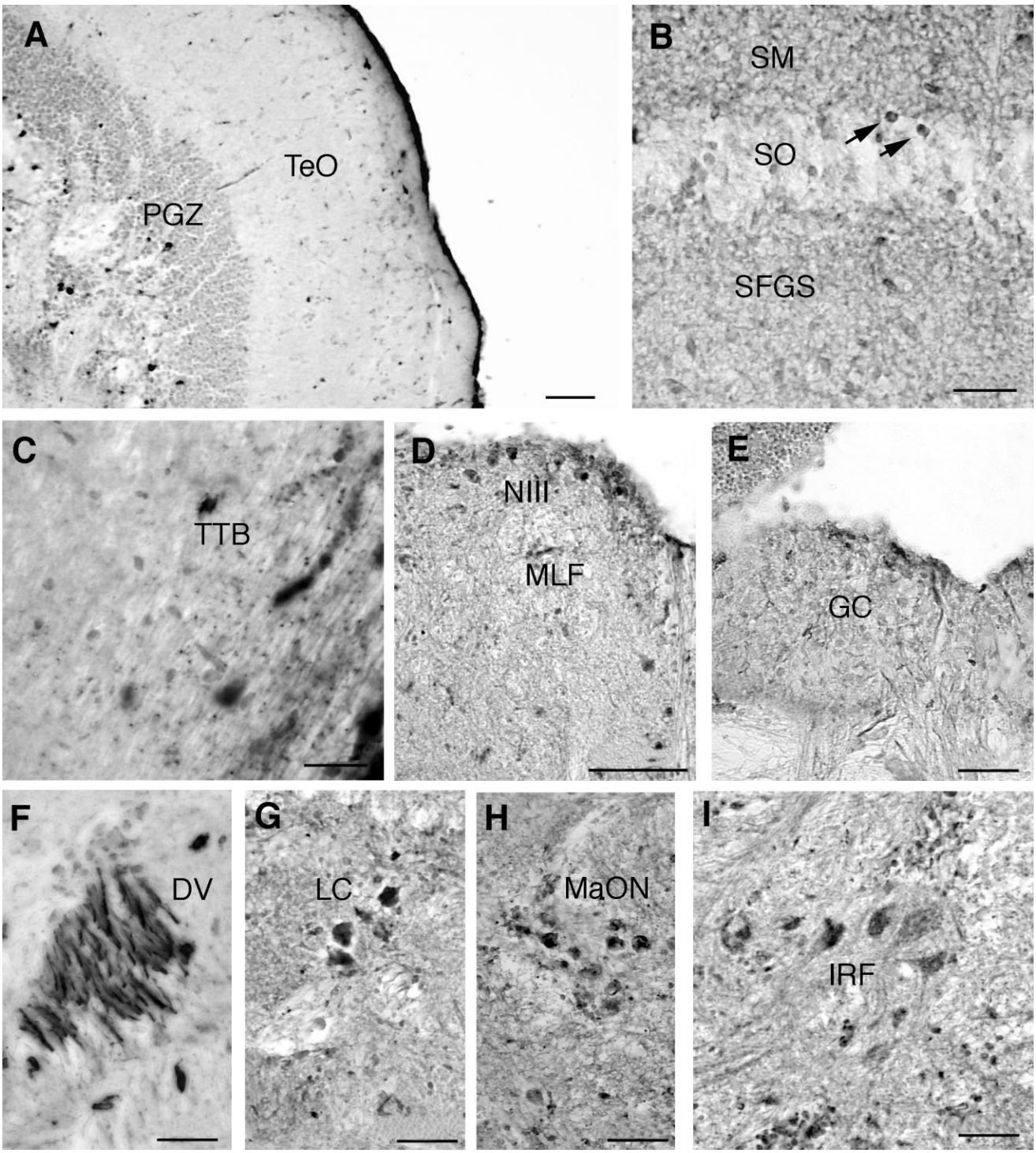

Fig. 5. Photomicrographs of transverse sections of the adult zebrafish mesencephalon and rhombencephalon. **A:** Immunoreactivity of the α_{2A}-ARs in the optic tectum and PGZ. **B:** High magnification showing stained α_{2A}-AR cells (arrows) in the SO layer of the optic tectum. **C:** α_{2A}-AR-labeled varicose fibers in the tectobulbar tract. **D:** Section showing α_{2A}-AR immunoreactivity in the oculomotor nucleus. **E:** α_{2A}-AR ir in the central gray. **F:** Detail of the strong α_{2A}-AR-immunostained fibers of the descending trigeminal root. **G:** Strong α_{2A}-AR-immunopositive neurons of the noradrenergic center of the brain, LC. **H:** Large α_{2A}-AR-labeled neurons in the magnocellular octaval nucleus. **I:** α_{2A}-AR-immunopositive small and large cells in the inferior reticular formation. For abbreviations see list. Scale bars = 0.05 mm in A,D; 0.02 mm in B,C,I; 0.03 mm in E–H.

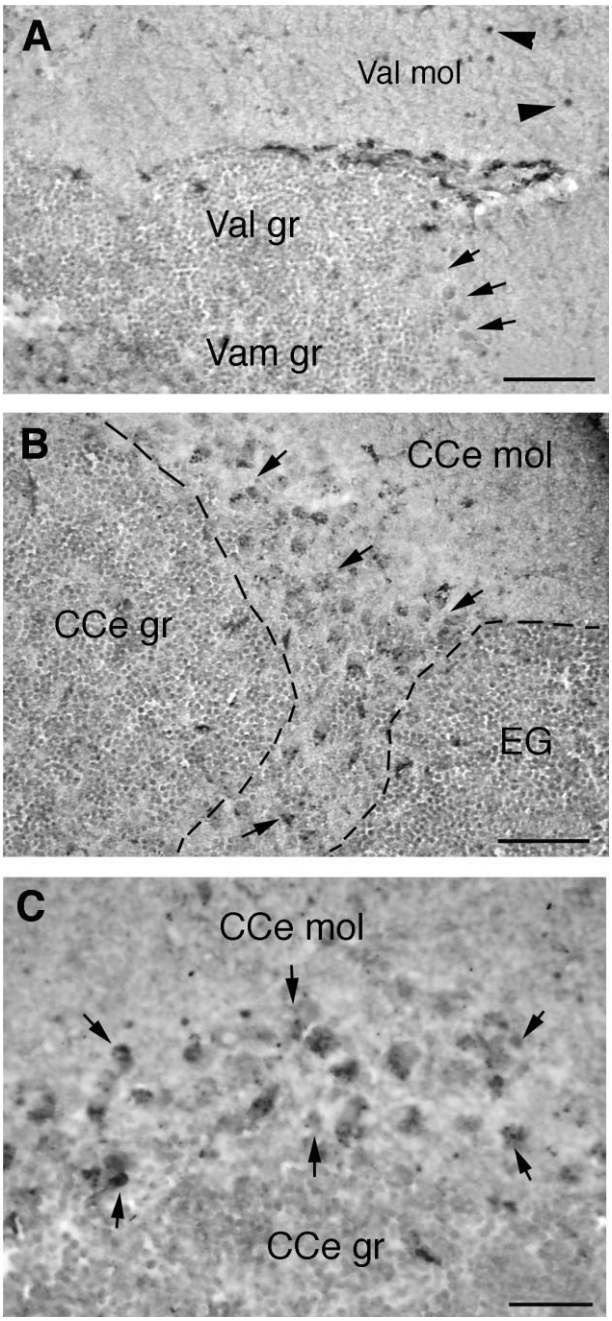

Fig. 6. Pattern of the α_{2A}-AR labeling in the cerebellum of the adult zebrafish. **A:** Immunopositive cells (arrows) of the ganglionic-Purkinje layer of the zebrafish valvula cerebellum. Arrowheads indicate round stained cells in the molecular layer of the valvula cerebellum. **B:** α_{2A}-AR expression in the Purkinje cell layer (arrows) in the corpus cerebellum. **C:** High-magnification photomicrograph showing the characteristic punctuate α_{2A}-AR immunolabeling on the Purkinje and eurydendroid cells (arrows) in the corpus cerebellum. For abbreviations see list. Scale bars = 0.05 mm in A,B; 0.03 mm in C.

zones (Zupanc et al., 2005; Ampatzis and Dermon, 2007). For this, we performed double-labeling experiments with the S-phase cell marker BrdU, but very few newborn cells were labeled for α_{2A}-AR, mainly in the optic tectum (TeO), and will not be treated here further.

α_{2A}-AR/HuC/D labeling. Double-label immunofluoresence of α_{2A}-AR and HuC/D antibody showed that, in several brain areas, neuronal cell somata expressed α_{2A}-ARs. Double-labeled cell expression of α_{2A}-ARs was found in the medial zone of the dorsal telencephalic area (Dm) and ventral nucleus of the ventral telencephalic area (Vv). Thalamus and hypothalamus showed no double-labeled cells (Hd; Fig. 7A). In rhombencephalon and mesencephalon, large neurons showed intense punctate labeling of α_{2A}-ARs. Such areas were the oculomotor nucleus (NIII; Fig. 7B), SRF (Fig. 7E), medial octavolateralis nucleus (MON), magnocellular octaval nucleus (MaON), griseum centrale (GC; Fig. 7D), and IRF. In cerebellum, the cells of the ganglionic layer stained with the neuronal marker HuC/D showed punctate labeling with α_{2A}-ARs (Fig. 7F). This punctate labeling of α_{2A}-AR in the HuC/D-positive cells resembled terminal axons. Whether the α_{2A}-AR labeling is intracellular or represents presynaptic receptors requires further elucidation at the ultrastuctural level. It is interesting to note that, in contrast, LC neurons were doubly labeled with Hu C/D and showed intense diffuse labeling of α_{2A}-ARs that extended over the entire surface of the cell bodies, but not the nucleus, indicating possible endocytoplasmic labeling (Fig. 7C). It is interesting to note that major tracts with Hu-positive axons were not labeled for α_{2A}-ARs.

α_{2A}-AR/PV labeling. Detailed observation of the double-labeling experiments showed no double-labeled cells of α_{2A}-AR and PV in the forebrain and the mesencephalon of adult zebrafish brain. However, in the forebrain, populations of cells expressing PV were closely associated with the α_{2A}-AR-positive neuropil (Fig. 7J). In the mesencephalon, periventricular gray zone of optic tectum (PGZ) included intermingled population of cells positive for PV and α_{2A}-ARs, but none was found to be double labeled. PV-positive fibers in TS and TeO were not associated with α_{2A}-AR-positive fibers. Double-labeled cells were found in the cerebellar areas but not in the molecular layer that was characterized by dense PV labeling. Specifically, some of the cell somata in the ganglionic cell layer that exhibited dense labeling for PV were also found to express α_{2A}-AR. In the rhombencephalic reticular formation nuclei, few spare PV-positive cells were observed in close apposition to the α_{2A}-AR-positive neurons, but no double-labeled cells were found.

α_{2A}-AR/GFAP labeling. Double-labeled fibers of α_{2A}-ARs and GFAP were revealed by immunohistofluorescence (Fig. 8A–G). Significant percentages of the processes expressing α_{2A}-ARs were found to be of glial nature. In adult zebrafish telencephalon, no double-labeled cells or fibers were found. In dorsal telencephalic areas, such as the medial zone of the dorsal telencephalic area (Fig. 8A), astroglial fibers extended centrifugal processes that came in contact with the pial surface. In diencephalon, the preoptic area (PPp), thalamic areas (CP, DP; Fig. 8C), pretectal area (PPv; Fig. 8C), posterior tuberculum (TPp), and hypothalamic areas, such as dorsal zone of the periventricular hypothalamus (Hd), included some glial fibers expressing α_{2A}-ARs. In contrast, in epithalamic areas, such as the habenular nuclei (Fig. 8B), which included many astroglial fibers, non was found to coexpress α_{2A}-ARs. In the mesencephalon, GFAP-positive radial glial fibers and cells in the periventricular gray zone of optic tectum (PGZ; Fig. 8D) were in close relation to the α_{2A}-AR-

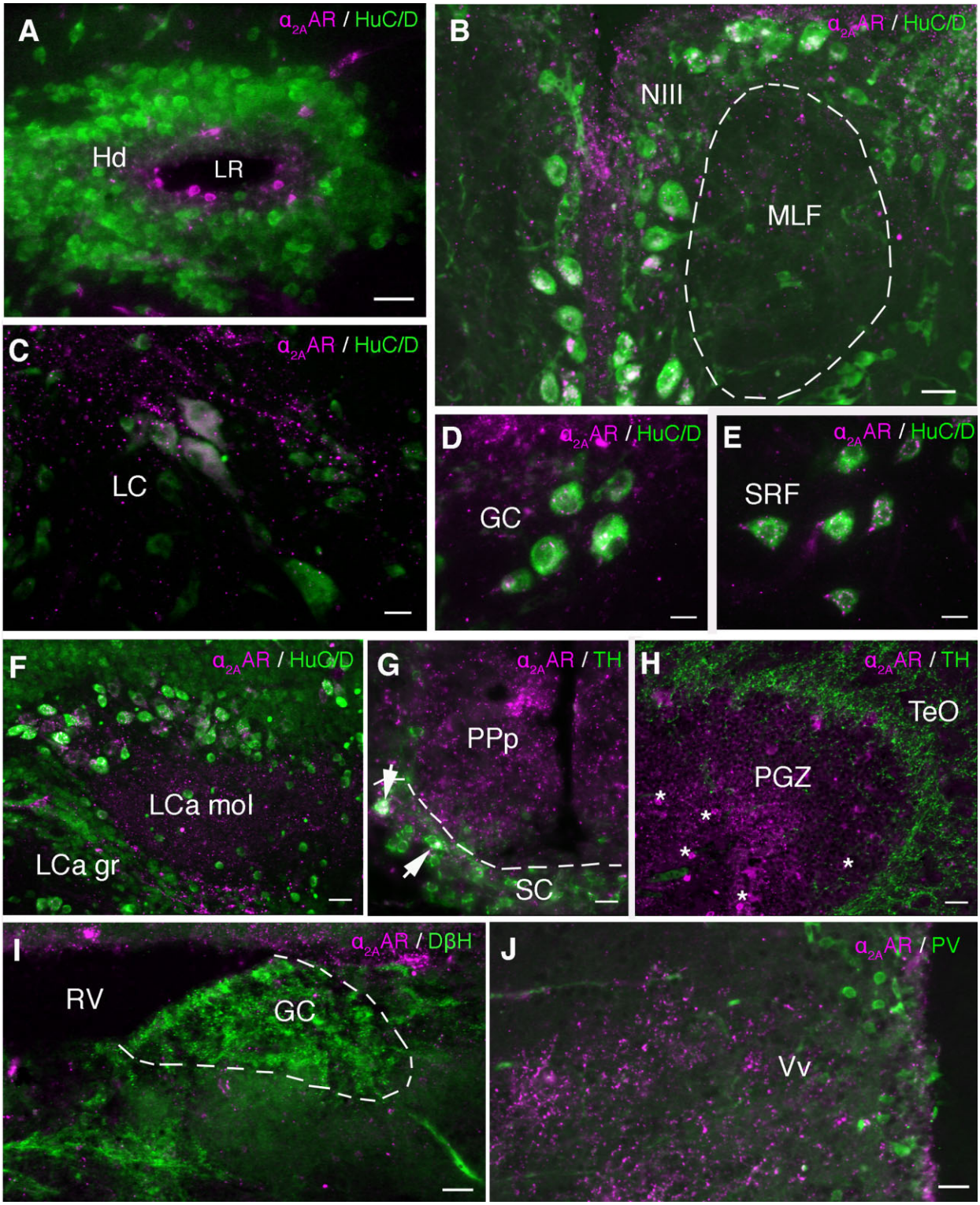

Fig. 7. Immunofluorescent microphotographs of selected transverse sections showing the localization of the neuronal marker HuC/D, tyrosine hydroxylase (TH), DβH, and parvalbumin (PV) with the α_{2A}-AR. **A–F:** Double labeling of the neuronal marker HuC/D (green) with the α_{2A}-AR (magenta) in selected coronal sections of the adult zebrafish brain. **G,H:** Images showing distribution of the TH and α_{2A}-AR in the diencephalic preoptic area and mesencephalon (arrows indicate α_{2A}-AR varicosities on TH cell somata). **I:** Colocalization of the DβH with α_{2A}-ARs in fibers in the central gray. **J:** Distinct localization of the PV and α_{2A}-ARs in the ventral telencephalic Vv. Double-labeled cells, appear white. Stars indicate stained blood vessels. For abbreviations see list. Scale bars = 0.02 mm.

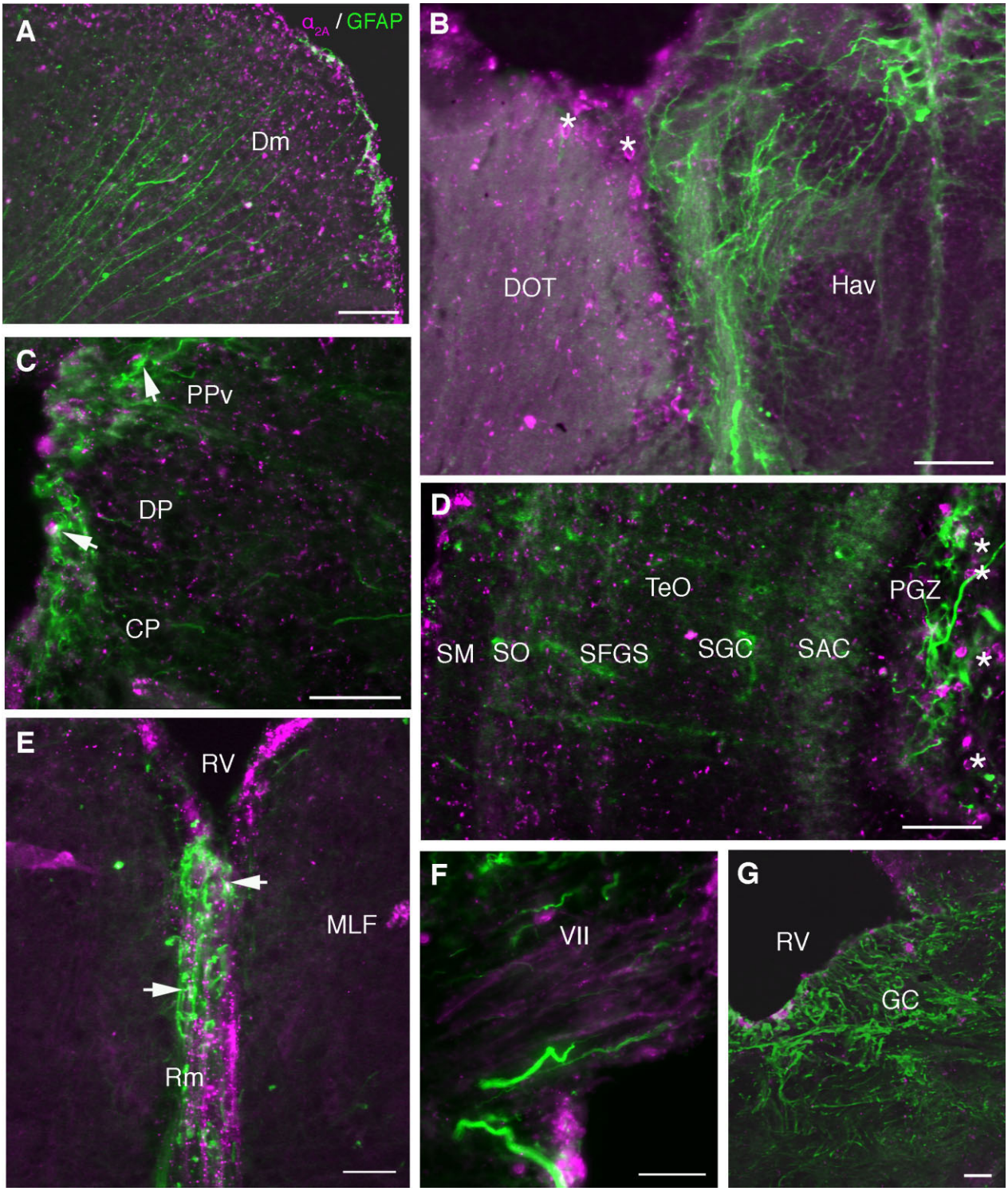

Fig. 8. Photomicrographs showing the distribution of the glial fibers (GFAP; green) and colocalization with α_{2A}-ARs (magenta) in the adult zebrafish brain. **A:** α_{2A}-AR- and GFAP-ir in the medial zone of the dorsal telencephalic area. **B:** GFAP fibers in the ventral habenular nucleus. **C:** α_{2A}-AR and GFAP immunofluoresence in the pretectal (PPv) and thalamic (DP, CP) nuclei. **D:** Glial and α_{2A}-AR ir in the optic tectum and periventricular gray zone of optic tectum. **E:** Double-labeled fibers in the rhombencephalon dorsal to the medial raphe nucleus. **F:** α_{2A}-AR-ir fibers and GFAP-positive fibers in the facial nerve. **G:** Immunostaining fibers with GFAP and α_{2A}-AR in the central gray. Arrows show double-labeled cells, appearing white. Stars indicate stained blood vessels. For abbreviations see list. Scale bars = 0.05 mm.

stained cells, but no double-labeled cells or fibers were detected. It is important to note that the population of α_{2A}-AR-positive small labeled cells in the OT and VOT were not labeled for GFAP nor for Hu C/D antibodies, so their identity is unclear. However, some OT α_{2A}-AR-positive fibers were found to be double labeled with GFAP. In addition, an important percentage of double-labeled processes was found in the rhombencephalic midline, at the level of the raphe nuclei (Kaslin and Panula, 2001). These were found originating close to the ventricle, running vertically, as in a waterfall (Fig. 8E). Caudally, GC included a high density of GFAP fibers, some of which (close to the ventricle) expressed α_{2A}-AR (Fig. 8G). In addition, nerves such as the VII nerve included separate populations of thick curved fibers expressing a high density of α_{2A}-AR or GFAP but not both (Fig. 8F).

α_{2A}-ARs in association with dopaminergic and noradrenergic cells and fibers

α_{2A}-AR/TH double-labeling experiments were performed to test the relation between adrenoceptors and dopaminergic neurons and fibers. TH catalyses the initial step in the catecholamine biosynthetic pathway and is expressed in most of the catecholaminergic neurons (Smeets and Gonzalez, 2000). In addition, we performed double-labeling experiments of α_{2A}-AR and DβH to investigate the relation of α_{2A}-ARs to the noradrenergic neurons and fibers. DβH, the enzyme involved in the synthesis of NA from dopamine, is a marker for noradrenergic and adrenergic neurons. The TH and DβH staining patterns observed in the present study via light microscopy were in agreement with the previously described cellular clusters of TH-positive cells (Kaslin and Panula, 2001). Specifically, noradrenergic neuropil revealed by DβH immunocytochemistry formed axons with en passant varicosities, as previously described (Anichtchik et al., 2006).

α_{2A}-AR/TH immunoreactivity. A close relationship with a complementary distribution pattern of TH and α_{2A}-AR was found, but no double-labeled cells were identified, with the exception of all (three to seven) of the LC cells that were double labeled. Although the locus coeruleus cell somata and initial segments of processes showed strong double labeling of α_{2A}-AR and TH immunoreactivity, TH reactivity extended further in the processes. In addition, in the suprachiasmatic nucleus (SC; Fig. 7G), varicosities expressing α_{2A}-ARs were found in close apposition to TH-positive cells, whereas, in optic tectum layers, TH-positive fibers were colocalized with α_{2A}-ARs (Fig. 7H).

α_{2A}-AR/DβH immunoreactivity. Double-labeling immunohistofluorescence performed in the adult zebrafish brain showed that only cell somata in the LC were double labeled. Specifically, the cell somata were double labeled for DβH and α_{2A}-ARs, in contrast to the TH/α_{2A}-AR double labeling that extended to proximal dendrites in addition to the cell somata. Double-labeled fibers were found around the ventral region of the rhombencephalic ventricle. These fibers extended radially through GC and unidentified adjacent areas (Fig. 7I), where varicosities expressing α_{2A}-AR were colocalized with DβH varicosity-bearing axons.

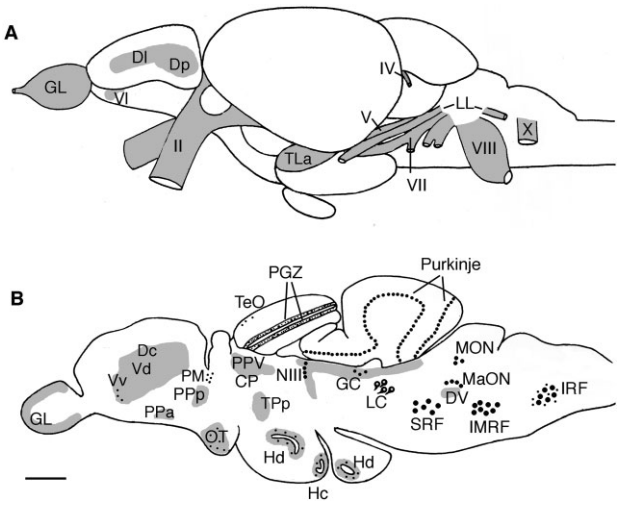

Fig. 9. Schematic sagittal drawings showing the main findings on the distribution of α_{2A}-AR-containing cells (solid circles) and fibers (gray area) in the adult zebrafish brain. **A:** Lateral view. **B:** Medial view close to the midline. Scale bar = 250 μm.

DISCUSSION

Methodological considerations

With the use of α_2-AR subtype-specific antibody (α_{2A}-AR), the differential distribution pattern of the α_{2A}-AR subtype, as well as its neuronal or glial localization, was studied in the zebrafish brain. The polyclonal primary anti-α_{2A}-AR antibody has been previously used in neuroanatomical studies in the CNS of many vertebrates (Hou et al., 2002; Manns et al., 2003; Ohshita et al., 2004; Modirrousta et al., 2005), including teleost fish (Zikopoulos and Dermon, 2005). In addition, the specificity of this antibody in teleost brain was determined by Western blot analysis of protein extracts in the red porgy (*Pagrus pagrus*; Zikopoulos and Dermon, 2005) and in the zebrafish brain (present study). In support, a previous study in zebrafish suggested the conservation of α_{2A}-AR compared with that in mammals (Ruuskanen et al., 2005b), by determining the expression of α_{2A}-ARs using mRNA RT-PCR in situ hybridization and receptor autoradiography. The present study is in general agreement with the previous report.

Pattern of α_{2A}-AR immunoreactivity in the adult zebrafish brain

In the mammalian (Bylund et al., 1994) and teleost (Zikopoulos and Dermon, 2005; Ruuskanen et al., 2005b) brains, the α_{2A}-AR is considered the main adrenoceptor subtype. The zebrafish α_{2A}-AR appears to have a pharmacological profile similar to that in the human (Bylund, 2005; Ruskannen et al., 2005a), and the α_{2A}-AR-ir elements showed a wide distribution in zebrafish brain, as expected from the pattern of the noradrenergic innervation in most vertebrates (for review see Smeets and Gonzalez, 2000). A summarizing schematic sagittal drawing highlights the major findings in the distribution pattern of α_{2A}-ARs in the adult zebrafish brain (Fig. 9). Most labeling was found close to the midline (in telencephalon

more prominent in the ventral telencephalic area), with a higher density in the posterior brain.

Neuronal α_{2A}-ARs were found in cell clusters of different cell sizes, for example, small in medial zone of dorsal telencephalic area, in ventral nucleus of ventral telencephalic area, in dorsal zone of periventricular hypothalamus, and in inferior reticular formation and large in LC, in oculomotor nucleus, in medial octavolateralis nucleus, in magnocellular octaval nucleus, in superior reticular formation, and in inferior reticular formation and Purkinje cell somata. In the present study in the zebrafish brain, perikaryal puncta associated with neuronal cells were characteristic for α_{2A}-AR-like immunoreactivity, often associated with cell bodies as well as neuropil. Studies in mammalian and avian brain using the α_{2A}-AR antibodies, showed similar discrete punctate labeling associated with neuronal cell somata (Guyenet et al., 1994; Talley et al., 1996). This type of punctate labeling in cell bodies has been associated to neuronal intracellular localization of α_{2A}-ARs (Talley et al., 1996). In agreement, confocal microscopy (Guyenet et al., 1994) demonstrated that labeling is largely intracellular. In addition to the punctate labeling pattern, diffuse α_{2A}-AR labeling characterized the zebrafish LC neurons that contained the only cell bodies with diffuse α_{2A}-AR labeling, leaving the nucleus empty, favoring the possible endoplasmatic localization the receptors. However, the present study cannot differentiate whether the most often observed punctate perikaryal labeling is intracellular or is associated with presynaptic terminals on the cell bodies labeled. The hypothesis of the possible presynaptic α_{2A}-AR localization on NA-releasing terminals, as in other vertebrates (Lopez et al., 1983; Milner et al., 1998), cannot be excluded. In support, mammalian noradrenergic neurons have been shown to express the A subtype in agreement with the proposed presynaptic role of this subtype (NA inhibition; Lee et al., 1998; Ihalainen and Tanila, 2002).

Significant immunoreactivity in the neuropil was related to glial processes in addition to the dendritic and axonal processes, in agreement with detailed reports on rat (Aoki et al., 1994; Talley et al., 1996; Milner et al., 1998) and monkey brain (Wang and Lidow, 1997). Most often α_{2A}-AR-positive fibers were a mixture of neuronal and glial processes. However, α_{2A}-ARs were associated not with astrocytic cell bodies but exclusively with their processes. Such astrocytic processes expressing α_{2A}-ARs were found mainly in the midline in preoptic (PPp), thalamic (CP, DP), and pretectal (PPv, TPp) areas and in the rhombencephalic midline at the level of medial raphe nucleus (Rm). In some cases, they were in association with the ventricle, such as in the dorsal zone of periventricular hypothalamus, in ventral part of periventricular pretectal nucleus, in dorsal posterior thalamic nucleus, in central posterior thalamic nucleus, and in GC. In cranial nerves, bundles of neuronal and astrocytic fibers were mixed, suggesting a regulating role of the α_{2A}-ARs in the nerve output. Indeed, glia–neuron cocultures showed that activation of α_{2A}-ARs influences synaptic communication, increasing extracellular calcium uptake (Muyderman et al., 1997), intracellular glutamine accumulation (Huang and Hertz, 2000), and glycogenolysis (Subbarao and Hertz, 1990). Furthermore, an ultrastuctural study in rat hippocampus demonstrated that astrocytic profiles are found near terminals forming asymmetric synapses (Milner et al., 1998). Therefore, α_{2A}-ARs may be strategically positioned in adjacent glia to influence neuronal communication (Glass et al., 2002).

Association of α_{2A}-AR immunoreactivity with noradrenergic and dopaminergic projections

Similarly to the case mammals, zebrafish LC provides most of the noraradrenergic projections to brain regions (Ma, 1997). The LC neurons in the zebrafish brain express TH and DβH reactivity (McLean and Fetcho, 2004; present study). In this study, LC neurons were identified in adult zebrafish isthmus by the dense expression of α_{2A}-ARs in their somata and proximal dendrites. This neurotransmitter profile further supports the homology of the teleost LC to its avian and mammalian counterparts. LC in teleosts innervates more rostral regions via two catecholaminergic pathways, the longitudinal catecholamine bundle and the periventricular catecholamine pathway (Ma, 1994b). The periventricular pathway gives rise to coarse terminal arbors with large but sparse varicosities, whereas the longitudinal catecholamine bundle gives rise to terminal plexuses with fine and dense fibers and varicosities (Ma, 1994b), resembling the present labeling texture. Moreover, the periventricular pathway innervates more dorsal structures, including the dorsal tegmentum, torus longitudinalis, posterior zone of dorsal telencephalic area, and dorsal zone of dorsal telencephalic and olfactory bulb, which in the present study exhibited low labeling of α_{2A}-ARs. In contrast, the longitudinal catecholamine pathway is prominent in more ventral structures, particularly in the hypothalamus and preoptic areas that included moderate to high densities of α_{2A}-ARs. Given the pattern and the texture of labeling, that is, dense fine punctate labeling, we speculate that α_{2A}-ARs are found mainly in varicosities of the longitudinal catecholamine bundle.

The occurrence of α_{2A}-ARs in the present study correlated well with MAO activity and mRNA (Anichtchik et al., 2006). Indeed, zebrafish hypothalamic areas, dorsal and medial raphe nuclei with intense enzyme histochemical/ immunohistochemical staining of MAO (Anichtchik et al., 2006), exhibited a high density of α_{2A}-AR immunoreactivity. Only few specific regions showed colocalization of α_{2A}-ARs and DβH, such as the LC and the GC, but the distribution of α_{2A}-ARs was in close association to the terminal areas of LC (Ma, 1994b). LC projection areas with high density of α_{2A}-ARs in cells and fibers were found to be the raphe nucleus, the interpeduncular nucleus, the torus semicircularis, the preoptic areas, and parts of the hypothalamus. A moderate density of α_{2A}-ARs was found in optic tectum, cerebellum, habenular complex, dorsomedial zone of area dorsalis telencephali, and olfactory bulb in agreement with their moderate levels of LC innervation (Ma, 1994b). In contrast, the torus longitudinalis was almost devoid α_{2A}-ARs, although it is moderately innervated by the LC. In the optic tectum, the precise topography of α_{2A}-ARs, with the dorsal and medial parts showing a higher density of positive cells and fibers, parallels the termination pattern of LC axons that enter the tectum medially, and the density of innervation is higher in the rostrodorsal than in the caudoventral tectum (Vanegas and Ito, 1983). This pattern resembles that of the TH-ir (dopaminergic) fibers and terminals in the optic tectum (Kaslin and Panula, 2001). In agreement, colocal-

ization experiments of α_{2A}-AR with TH, similarly to the DβH experiments, outlined the large cell somata of LC neurons. That is, noradrenergic LC neurons expressing α_{2A}-ARs exhibited TH activity in the zebrafish.

Mismatches between receptor and transmitter localization have been reported in many species (Herkenham, 1987), and detection of α_{2A}-AR-like immunoreactivity in areas with no noradrenergic input may indicate the presence of adrenergic heteroreceptors that function in volume transmission (Fuxe and Agnati, 1985). In addition, α_{2A}-ARs have been found on non-noradrenergic terminals in previous studies (Milner et al., 1998), for example, modulating calcium-dependent release from terminals containing γ-aminobutyric acid, glutamate, and serotonin (Consolo et al., 1982; Maura et al., 1988; Bickler and Hansen, 1996) or located on cholinergic terminals (Heider et al., 1997).

It is interesting that essentially all sites with a high density of α_{2A}-ARs contain catecholaminergic, serotonergic, or histaminergic fibers (Ma, 1994a; Kaslin and Panula, 2001), e.g., catecholaminergic projections from the posterior tubercle to the ventral telencephalic area have been demonstrated experimentally in zebrafish (Rink and Wullimann, 2001, 2002), and both areas exhibited dense labeling of α_{2A}-AR-positive fibers. In addition, the medial and dorsal raphe nuclei that are known to include serotonergic neurons (Kaslin and Panula, 2001) exhibited α_{2A}-AR-positive fibers. Studies in teleosts have shown the close interaction of the dopaminergic and noradrenergic systems (Meek et al., 1993; Smeets and Gonzalez, 2000; Kaslin and Panula, 2001). Our findings support a close complementary localization of α_{2A}-ARs with dopaminergic (TH-positive) neuronal somata and fibers. However, only in specific areas, such as LC, optic tectum, and suprachiasmatic nucleus, did the TH cells and fibers express α_{2A}-ARs, suggesting a possible presynaptic localization of the α_{2A}-ARs.

Comparison with other vertebrates and functional implications

Autoradiographic, in situ hybridization, and immunohistochemical studies suggest that the α_{2A}-AR subtype is the most prominent type among α_2-ARs in the mammalian and avian brain (Nicholas et al., 1993; Talley et al., 1996). Structural and pharmacological properties (Ruuskanen et al., 2005a,b) as well as localization of α-adrenergic subtypes in the adult zebrafish showed marked conservation compared with mammals, with the α_{2A}-ARs distributed in the CNS and in peripheral organs (Ruuskanen et al., 2005b). The distribution of α_{2A}-ARs in the adult zebrafish brain and the close association with the noradrenergic and dopaminergic systems suggest that the catecholamine influences on behavioral output (Winberg and Nilsson, 1992) are partially mediated by the α_{2A}-ARs. Such influences, based on the close ties with neurohormonal systems, potentially regulate developmental, reproductive, and agonistic processes (Peter and Fryer, 1983; Parent, 1984).

Telencephalon. It is difficult to make comparisons of the teleost telencephalon, characterized by different degrees of eversion between teleosts, with the avian and mammalian telencephalon, which develops by evagination of pallial masses. However, homologies have been proposed on the basis of ontogenetic, chemoarchitectonic, and connectional features (Northcutt and Bradford, 1980; Butler and Hodos, 1996; Wulliman and Rink, 2002). Among dorsal telencephalon, which is considered pallial, moderate levels of cells and fibers expressing α_{2A}-ARs were found in midline regions of medial zone of dorsal telencephalic area (pallial amygdala; Bradford and Northcutt, 1983) and posterior zone of dorsal telencephalic area (olfactory pallium; Wulliman and Mueller, 2004). It is of particular interest that lesion of this particular subregion of medial zone of dorsal telencephalic area (ventromedial midline) impaired performance of shuttle avoidance tasks (Portavella et al., 2002), involving α_{2A}-ARs in aversive learning in zebrafish as in birds (Stamatakis et al., 1998). The adjacent dorsolateral zone (Dl), involved in spatial-temporal learning and memory processes in teleosts, resembling hippocampal functions of other vertebrates (Portavella et al., 2002; Rodriguez et al., 2002), included moderate levels AR-expressing fibers, comparable to those of the caudoventral region of mammalian hippocampus (Unnerstall et al., 1984). In addition, α_2-ARs in large fibers of the central zone of dorsal telencephalic area, in agreement with autoradiographic study in the adult zebrafish brain (Ruuskanen et al., 2005b), possibly suggest their regulatory role in the communication between the telencephalon and the precerebellar and auditory (torus semicircularis) centers (Ito et al., 1982; Striedter, 1990; Wullimann and Meyer, 1993; Imura et al., 2003; Folgueira et al., 2004).

The density of α_{2A}-ARs is higher in the ventral telencephalon, which is considered comparable to the subpallium of land vertebrates (Reiner and Northcutt 1992; Wulliman and Mueller, 2004). This pattern resembles that of birds and mammals (Dermon and Kouvelas, 1988, 1989; Talley et al., 1996). In agreement with studies in other vertebrates, its ventral tier in zebrafish (Vv, Vl) is particularly rich in fibers with α_{2A}-ARs. These areas correspond to the septal formation, which is strongly connected to preoptic region/midline hypothalamus (Rink and Wulliman, 2004), areas with high noradrenergic input (Ma, 1994b). In contrast, the dorsal nucleus of ventral telencephalic area and the supracommisural nucleus of ventral telencephalic area, resembling the mammalian striatal areas, exhibited low α_{2A}-AR labeling. This finding further supports the proposed homology and adds to our knowledge of the neurochemical profile of these areas (Rink and Wulliman, 2004).

Diencephalon. The α_{2A}-AR distribution pattern in most of the zebrafish diencephalic areas is comparable to that obtained in other studies of teleost fish (Zikopoulos and Dermon, 2005), including the zebrafish (Ruuskanen et al., 2005b), as well as in studies of avian (Ball et al., 1989; Dermon and Kouvelas, 1989; Fernandez-Lopez et al., 1997) and mammalian (Unnerstall et al., 1984) brain. Specifically, the presence of high density of α_{2A}-AR in the zebrafish hypothalamic areas is in agreement with mammalian (Unnerstall et al., 1984), avian (Ball et al., 1989; Dermon and Kouvelas, 1989; Fernandez-Lopez et al., 1997), and teleost (Ruuskanen et al., 2005b; Zikopoulos and Dermon, 2005) studies. In particular the dorsal zone of periventricular hypothalamus, suggested to be involved in the sex change in hermaphrodite fish (Zikopoulos et al., 2001), contained fibers expressing a high density of α_{2A}-ARs.

Moderate to high density of α_{2A}-ARs fibers and cells characterized the posterior preoptic area, relating α_{2A}-ARs to known functions of the preoptic area in fish, such

as reproductive behavior, temperature regulation, and neuroendocrine regulation (Butler and Hodos, 1996; Wullimann et al., 1996).

Mesencephalon. Sensory integration centers, the optic tectum (mostly visual input; superior colliculus in mammals; Butler and Hodos, 1996) and the semicircular torus (mostly acoustic and lateral line input; inferior colliculus in mammals; Butler and Hodos, 1996), exhibited moderate levels of α_{2A}-AR labeling; that is, superficial tectal layers contained higher numbers of medium-sized α_{2A}-AR-ir neurons and fibers than deeper periventricular layer (SGP), in agreement with previous study (Ruuskanen et al., 2005b). This pattern is similar to that described for birds (Ball et al., 1989; Dermon and Kouvelas, 1989; Fernandez-Lopez et al., 1997) and mammals (Palacios and Kuhar, 1980; Unnerstall et al., 1984), highlighting a possibly similar role of the noradrenergic system in sensory modulation and integration among vertebrates. The fact that the dorsomedial tectal portion, the origin of the tectal projections to the nucleus rostrolateralis that is involved in feeding (Wullimann et al., 1996; Saidel and Butler, 1997), included a high density of α_{2A}-AR supports the idea that α_{2A}-ARs play a role in the visual and motor control of feeding. In addition, the presence of α_{2A}-ARs in the periventricular gray zone of optic tectum and optic tract further supports an influence on retinotectal communication.

Rhombencephalon. In teleosts, most noradrenergic cell somata are confined to a small rhombencephalic region (Ekström et al., 1986; Sas et al., 1990; Ma, 1994b), homologous to the mammalian LC (Kaslin and Panula, 2001). The LC is the most ancient and consistent noradrenergic cell groups in the CNS of vertebrates (Parent, 1984; Ma, 1994a). The LC in zebrafish contains only few large neurons (3–10; Ma, 1994a) that, similarly to mammals, provide most of the noradrenergic input to the brain regions (Ma, 1997). In mammals, it has been involved in many functions, including the mediation of orientation, arousal states, neuronal plasticity, and learning and memory (Foote et al., 1983). At present, the teleostean LC is defined as noradrenergic by its coexpression of TH and DβH reactivity (Kaslin and Panula, 2001). The high density α_{2A}-ARs in the cell bodies and initial segment of processes of LC neurons provides further new evidence for identifying the zebrafish LC and for establishing homology to the avian and mammalian LC.

In the medulla, the descending trigeminal root (DV) included a high density of α_{2A}-AR-positive fibers, and the longitudinal fiber tract systems, the medial and lateral longitudinal fascicle, and the secondary gustatory tract (SGT), known to include dopaminergic cells (Ma, 1997), were moderately labeled for α_{2A}-ARs fibers and cells. The vagal lobe (LX), known to be related to the bulbospinal tract (TBS) with the dendrites of its neurons wrapping around some fascicles of this tract (Ma, 1997), included a high density of positive fibers, but only few medium-sized cells expressed α_{2A}-ARs. The medial octavolateralis nucleus, which receives first-order mechanosensory input from the lateral line, is one of the most heavily catecholamine innervated structure in the medulla (Ma, 1997) and receives its innervation from the longitudinal catecholamine bundle. Most of its large cells as well as fibers expressed α_{2A}-ARs. The oculomotor nucleus (NIII) and nucleus of medial longitudinal fascicle (NMLF), with dense labeling of α_{2A}-ARs, are targets of pronominally contralateral output of the teleostean cerebellum (Wullimann et al., 1996). Taken together, the above-mentioned medullary catecholaminergic cell groups (Ma, 1997) were found to express α_{2A}-ARs, providing strong evidence of their role specifically in the longitudinal catecholamine pathway.

Cerebellum. The observed adrenoceptor laminar localization pattern in zebrafish cerebellum was in good agreement with its innervation pattern by the LC fibers previously described for teleosts (Ekström et al., 1986; Ma, 1994b). Specifically, it is known that innervation patterns of LC fibers in the corpus (CC) and the valvula cerebellaris (Va) are identical and that the highest density of noradrenergic fibers is found in the Purkinje cell layer, with the granular layer containing a relatively low density, whereas the molecular layer is uninnervated (Ma, 1994b), matching the MAO activity (Anichtchik et al., 2006). Moreover, the pattern in α_{2A}-ARs in the zebrafish cerebellum was consistent with that in avian (Dermon and Kouvelas, 1988, 1989; Fernandez-Lopez et al., 1997) and mammalian (Palacios and Kuhar, 1980; Unnerstall et al., 1984; Scheinin et al., 1994) cerebellum.

CONCLUSIONS

The functional importance of the α_{2A}-ARs in neuronal cell bodies and fibers as well as glial processes in adult zebrafish brain is not known at present. However, the close association of these receptors with the ventricular milieu of the isthmus and the pons supports their role in autonomic functions. In addition, their presence in a number of first- and second-order sensory structures and nerve nuclei neurons and highly varicose processes suggests the α_{2A}-AR involvement in sensory regulation and integration.

LITERATURE CITED

Alonso JR, Arevalo R, Brinon GJ, Lara J, Weruaga E, Aijon J. 1992. Parvalbumin immunoreactive neurons and fibers in the teleost cerebellum. Anat Embryol 184:355–361.

Alumni A, Vaccari S, Torcia S, Meomartini ME, Nicorta A, Alfei L. 2005. Characterization of glial fibrillary acidic protein and astroglial architecture in the brain of a continuously growing fish, the rainbow trout. Eur J Histochem 49:157–166.

Ampatzis K, Dermon CR. 2007. Sex differences in adult cell proliferation within the zebrafish (*Danio rerio*) cerebellum. Eur J Neurosci 25:1030–1040.

Anichtchik O, Sallinen V, Peitsaro N, Panula P. 2006. Distinct structure and activity of monoamine oxidase in the brain of zebrafish (*Danio rerio*). J Comp Neurol 498:593–610.

Aoki C, Go C-G, Venkatesan C, Kurose H. 1994. Perikaryal and synaptic localization of α(2A)-adrenergic receptor-like immunoreactivity. Brain Res 650:181–204.

Bachman GL, Uhlen S, Herman CA. 1998. Localization and changes in distribution of brain alpha 2- and beta-adrenoceptors in response to acclimation state in the American bullfrog (*Rana catesbeiana*). Gen Comp Endocrinol 110:166–174.

Ball GF, Nock B, McEwen BS, Balthazart J. 1989. Distribution of alpha 2-adrenergic receptors in the brain of the Japanese quail as determined by quantitative autoradiography: implications for the control of sexually dimorphic reproductive processes. Brain Res 491:68–79.

Barami K, Iversen K, Furneaux H, Goldman SA. 1995. Hu protein as an early marker of neuronal phenotypic differentiation by subependymal zone cells of the adult songbird forebrain. J Neurobiol 28:82–101.

Bickler PE, Hansen BM. 1996. α_2-Adrenergic agonists reduce glutamate release and glutamate receptor-mediated calcium changes in hippocampal slices during hypoxia. Neuropharmacology 35:679–687.

Bodega G, Suarez I, Rubio M, Fernandez B. 1990. Distribution and char-

acteristics of the different astroglial cell types in the adult lizard (*Lacerta lepida*) spinal cord. Anat Embryol 181:567–575.

Bodega G, Suarez I, Rubio M, Villaba RM, Fernandez B. 1993. Astroglial pattern in the spinal cord of the adult barbel (*Barbus comiza*). Anat Embryol 187:385–395.

Bodega G, Suarez I, Rubio M, Fernandez B. 1994. Ependyma: phylogenetic evolution of glial fibrillary acidic protein (GFAP) and vimentin expression in vertebrate spinal cord. Histochemistry 102:113–122.

Bradford MR Jr, Northcutt RG. 1983. In: Northcutt RG, Davis RE, editors. Fish neurobiology, vol 2. Ann Arbor, MI: The University of Michigan Press. p 117–163.

Bu J, Sathyendra V, Nagykery N, Geula C. 2003. Age-related changes in calbindin-D28k, calretinin, and parvalbumin immunoreactive neurons in the human cerebral cortex. Exp Neurol 182:220–231.

Butler AB, Hodos W. 1996. Comparative vertebrate neuroanatomy: evolution and adaption. New York: Wiley-Liss.

Bylund DB. 1988. Subtypes of α_2-adrenoceptors: pharmacological and molecular biological evidence converge. Trends Pharmacol Sci 9:356–361.

Bylund DB. 2005. Alpha-2 adrenoceptor subtypes: are more better? Br J Pharmacol 144:159–160.

Bylund DB, Eikenberg DC, Hieble JP, Langer SZ, Lefkowitz RJ, Minneman KP, Molinoff PB, Ruffolo RR, Trendelenburg U. 1994. International union of Pharmacology nomenclature of adrenoceptors. Pharmacol Rev 46:121–136.

Byrd CA, Brunjes PC. 2001. Neurogenesis in the olfactory bulb of adult zebrafish. Neuroscience 105:793–801.

Celio MR. 1990. Calbindin D-28k and parvalbumin in the rat nervous system. Neuroscience 35:375–475.

Celio MR, Baier W, de Viragh P, Scharer L, Gerday C. 1988. Monoclonal antibodies directed against the calcium binding protein parvalbumin. Cell Calcium 9:81–86.

Ciriello J, Caverson MM, Polosa C. 1989. The central neural organization of cardiovascular control. In: Progress in brain research, vol 81. Amsterdam/New York: Elsevier.

Civantos Calzada B, Aleixandre de Artinano A. 2001. Alpha-adrenoceptor subtypes. Pharmacol Res 44:195–208.

Consolo S, Ladinsky H, Forloni GL, Grombi P. 1982. Modulation of the hippocampal α-adrenoceptor population by lesion of the serotonergic raphe-hippocampal pathway in rats. Life Sci 30:1113–1119.

Crespo C, Porteros A, Arevalo R, Brinon JG, Aijon J, Alonso JR. 1999. Distribution of parvalbumin immunoreactivity in the brain of tench (*Tinca tinca* L., 1758). J Comp Neurol 413:549–571.

Dermon CR, Kouvelas ED. 1988. Binding properties, regional ontogeny and localization of adrenergic receptors in chick brain. Int J Dev Neurosci 6:471–482.

Dermon CR, Kouvelas ED. 1989. Quantitative analysis of the localization of adrenergic binding sites in chick brain. J Neurosci Res 23:297–303.

Docherty RJ. 1998. Subtypes of functional a1- and a2-adrenoceptors. Eur J Pharmacol 361:1–15.

Ekström P, Reschke M, Steinbusch H, Van Veen T. 1986. Distribution of noradrenaline in the brain of the teleost *Gasterosteus aculeatus* L.: an immunohistochemical analysis. J Comp Neurol 254: 297–313.

Eng LF, Ghirnikar RS, Lee YL. 2000. Glial fibrillary acidic protein: GFAP—thirty one years (1969–2000). Neurochem Res 25:1439–1451.

Fernandez-Lopez A, del Arco C, Gonzalez AM, Gomez T, Calvo P, Pazos A. 1990. Autoradiographic localization of alpha 2-adrenoceptors in chick brain. Neurosci Lett 120:97–100.

Fernandez-Lopez A, Revilla V, Candelas MA, Gonzalez-Gil J, Diaz A, Pazos A. 1997. A comparative study of alpha2- and beta-adrenoceptor distribution in pigeon and chick brain. Eur J Neurosci 9:871–883.

Folgueira M, Anadón R, Yáñez J. 2004. An experimental study of the connections of the telencephalon in the rainbow trout (*Oncorhynchus mykiss*). II. Dorsal area and preoptic region. J Comp Neurol 480:204–233.

Foote SL, Bloom FE, Aston-Jones G. 1983. Nucleus locus coeruleus: new evidence of anatomical and physiological specificity. Physiol Rev 63: 844–914.

Fuxe K, Agnati LF. 1985. Receptor-receptor interactions in the central nervous system. A new integrative mechanism in synapses. Med Res Rev 5:441–482.

Glass MJ, Colago EE, Pickel VM. 2002. Alpha-2A-adrenergic receptors are present on neurons in the central nucleus of the amygdala that project to the dorsal vagal complex in the rat. Synapse 46:258–268.

Goodman RL, Havern RL, Whisnant CS. 1996. Alpha adrenergic neurons inhibit luteinizing hormone pulse amplitude in breeding season ewes. Biol Reprod 54:380–386.

Grandel H, Kaslin J, Ganz J, Wenzel I, Brand M. 2006. Neural stem cells and neurogenesis in the adult zebrafish brain: origin, proliferation dynamics, migration and cell fate. Dev Biol 195:263–277.

Guo S, Wilson SW, Cooke S, Chitnis AB, Driever W, Rosenthal A. 1999. Mutations in the zebrafish unmask shared regulatory pathways controlling the development of catecholaminergic neurons. Dev Biol 208: 473–487.

Guyenet PG, Stornetta RL, Riley T, Norton FR, Rosin DL, Lynch KR. 1994. Alpha2A-adrenergic receptors are present in lower brainstem catecholaminergic and serotonergic neurons innervating spinal cord. Brain Res 638:285–294.

Harrison JK, Pearson WR, Lynch KR. 1991. Molecular characterization of a1- and a2-adrenoceptors. Trends Pharmacol Sci 12:62–67.

Heider M, Schliebs R, Roßner S, Bigl V. 1997. Basal forebrain cholinergic immunolesion by ^{192}IgG-saporin: Evidence for a presynaptic location of subpopulations of α_2-and β-adrenergic as well as 5-HT(2A) receptors on cortical cholinergic terminals . Neurochem Res 22:957–966.

Hein L, Kobilka BK. 1997. Adrenergic receptors: from molecular structure to in vivo function. Trends Cardiovasc Med 7:137–145.

Herkenham M. 1987. Mismatches between neurotransmitter and receptor localizations in brain: observations and implications. Neuroscience 23: 1–38.

Holmgren S, Nilsson S. 1982 .Neuropharmacology of adrenergic neurons in teleost fish. Comp Biochem Physiol C72:289–302.

Hou YP, Manns ID, Jones BE. 2002. Immunostaining of cholinergic pontomesencephalic neurons for alpha 1 versus alpha 2 adrenergic receptors suggests different sleep-wake state activities and roles. Neuroscience 114:517–521.

Huang R, Hertz L. 2000. Receptor subtype and dose dependence of dexmedetomidine-induced accumulation of [^{14}C]glutamine in astrocytes suggests glial involvement in its hypnotic-sedative and anesthetic-sparing effects. Brain Res 873:297–301.

Ihalainen JA, Tanila H. 2002. In vivo regulation of dopamine and noradrenaline release by α_{2A}-adrenoceptors in the mouse prefrontal cortex. Eur J Neurosci 15:1789–1794.

Imura K, Yamamoto N, Sawai N, Yoshimoto M, Yang CY, Xue HG, Ito H. 2003. Topographical organization of an indirect telencephalo-cerebellar pathway through the nucleus paracommissuralis in a teleost, *Oreochromis niloticus*. Brain Behav Evol 61:70–90.

Ito H, Murakami T, Morita Y. 1982. An indirect telencephalo-cerebellar pathway and its relay nucleus in teleost. Brain Res 249:1–13.

Kable JW, Murrin LC, Bylund DB. 2000. In vivo gene modification elucidates subtype-specific functions of a2-adrenergic receptors. J Pharmacol Exp Ther 293:1–7.

Kaslin J, Panula P. 2001. Comparative anatomy of the histaminergic and other aminergic systems in zebrafish (*Danio rerio*). J comp Neurol 440:342–377.

Kaslin J, Nystedt JM, Östergård M, Peitsaro N, Panula P. 2004. The orexin/hypocretin system in zebrafish is connected to the aminergic and cholinergic systems. J Neurosci 24:2678–2689.

Katayama H, Morshita F, Matsushima O, Fujimoto M. 1999. Beta adrenergic subtypes in melanophores of the marine gobies *Tridentiger trigonocephalus* and *Chasmichthys gulosus*. Pigment Cell Res 12:206–217.

Lee A, Rosin DL, Van Bockstaele EJ. 1998. α_{2A}-Adrenergic receptors in the rat nucleus locus coeruleus: subcellular localization in catecholaminergic dendrites, astrocytes, and presynaptic axon terminals. Brain Res 795:157–169.

Leibowitz SF, Jhanwar-Uniyal M, Dvorkin B, Makman MH. 1982. Distribution of alpha-adrenergic, beta-adrenergic and dopaminergic receptors in discrete hypothalamic areas of rat. Brain Res 233:97–114.

Levitt P, Rakic P. 1980. Immunoperoxidase localization of glial fibrillary acidic protein in radial glial cells and astrocytes of the developing rhesus monkey brain. J Comp Neurol 193:815–840.

Lopez HP, Kiss D, Da Prada M, Haeusler G. 1983. Effects of clonidine on the rate of noradrenaline turnover in discrete areas of the rat central nervous system. Naunyn Schmiedeberg Arch Pharmacol 323:307–314.

Lorenz W, Lomasney JW, Collins S, Regan JW, Caron MG, Lefkowitz RJ. 1990. Expression of three a2-adrenergic receptor subtypes in rat tissues: implications for a2-receptor classification. Mol Pharmacol 38: 599–603.

Ma PM. 1994a. Catecholaminergic systems in the zebrafish. I. Number, morphology and histochemical characteristics of neurons in the locus coeruleus. J Comp Neurol 344:242–255.

Ma PM. 1994b. Catecholaminergic systems in the zebrafish. II. Projection pathways and pattern of termination of the locus coeruleus. J Comp Neurol 344: 256–269.

Ma PM. 1997. Catecholaminergic systems in the zebrafish III. Organization and projection pattern of medullary dopaminergic and noradrenergic neurons. J Comp Neurol 381:411–427.

Ma PM. 2003. Catecholaminergic systems in the zebrafish. IV. Organization and projection pattern of dopaminergic neurons in the diencephalon. J Comp Neurol 460:13–37.

Maler L, Ellis WG. 1987. Inter-male aggressive signals in weakly electric fish are modulated by monoamines. Behav Brain Res 25:75–81.

Manns ID, Lee MG, Modirrousta M, Hou YP, Jones BE. 2003. Alpha 2 adrenergic receptors on GABAergic, putative sleep-promoting basal forebrain neurons. Eur J Neurosci 18:723–727.

Marrone RL, Pray SL, Bridges CC. 1966. Norepinephrine elicitation of aggressive display responses in *Betta splendens*. Psychon Sci 5:207–208.

Marusich MF, Furneaux HM, Henion PD, Weston JA. 1994. Hu neuronal proteins are expressed in proliferating neurogenic cells. J Neurobiol 25:143–155.

Maura G, Pittaluga A, Ulivi M, Raiteri M. 1988. Enhancement of endogenous GABA release from rat synaptosomal preparations is mediated by α_2-adrenoceptors pharmacologically different from α_2-autoreceptors. Eur J Pharmacol 157:23–29.

McLean DL, Fetcho JR. 2004. Ontogeny and innervation patterns of dopaminergic, noradrenergic, and serotonergic neurons in larval zebrafish. J Comp Neurol 480:38–56.

Meek J, Joosten HW, Hafmans TG. 1993. Distribution of noradrenaline immunoreactivity in the brain of the mormyrid teleost *Gnathonemus petersii*. J Comp Neurol 328:145–160.

Milner TA, Lee A, Aicher SA, Rosin DL. 1998. Hippocampal α(2A)-adrenergic receptors are located predominantly presynaptically but are also found postsynaptically and in selective astrocytes. J Comp Neurol 395:310–327.

Modirrousta M, Mainville L, Jones BE. 2005. Orexin and MCH neurons express c-Fos differently after sleep deprivation vs. recovery and bear different adrenergic receptors. Eur J Neurosci 21:2807–2816.

Morris MJ, Elghozi JL, Dausse JP, Meyer P. 1981. Alpha 1- and alpha 2-adrenoceptors in rat cerebral cortex: effect of frontal lobotomy. Naunyn Schmiedeberg Arch Pharmacol 316:42–44.

Mueller T, Wullimann MF. 2002. BrdU-, *neuroD* (*nrd*)- and Hu-studies reveal unusual non-ventricular neurogenesis in the postembryonic zebrafish forebrain. Mech Dev 117:123–135.

Mueller T, Vernier P, Wullimann MF. 2004. The adult central nervous cholinergic system of a neurogenetic model animal, the zebrafish *Danio rerio*. Brain Res 1011:156–169.

Muyderman H, Hansson E, Nilsson M. 1997. Adrenoceptor-induced changes of intracellular K^+ and Ca^{2+} in astrocytes and neurons in rat cortical primary cultures. Neurosci Lett 238:33–36.

Naaser Y, Ho W, Sharkey KA. 2006. Distribution of adrenergic receptors in the enteric nervous system of the guinea pig, mouse, and rat. J Comp Neurol 495:529–53.

Nechaev IV. 1991. Catecholaminergic regulation of social behaviour in fish. In: Winlow W, Vinogradova OS, Sakharov DA, editors. Signal molecules and behavior. Manchester: Manchester University Press. p 191–198.

Nicholas AP, Pieribone V, Hokfelt T. 1993. Distributions of mRNAs for alpha-2 adrenergic receptor subtypes in rat brain: an in situ hybridization study. J Comp Neurol 328:575–594.

Nielsen AL, Jorgensen AL. 2003. Structural and functional characterization of the zebrafish gene for glial fibrillary acidic protein. Gene 310: 123–132.

Northcutt RG, Bradford MR Jr. 1980. New observations on the organization and evolution of the telencephalon of actinopterygian fishes. In: Ebbesson SOE, editors. Comparative neurology of the telencephalon. New York: Plenum Press. p 41–98.

Ohshita N, Nakajo N, Takemura M. 2004. Characteristics of the trigeminal depressor response in cats. J Neurosci Res 76:891–901.

Palacios JM, Kuhar MJ. 1980. Beta-adrenergic-receptor localization by light microscopic autoradiography. Science 208:1378–1380.

Parent A. 1983. The monoamine-containing neuronal systems in the teleostean brain. In: Davis RE, Northcutt RG, editors. Fish neurobiology, vol 2. Ann Arbor. MI: University of Michigan Press. p 285–316.

Parent A. 1984. Functional anatomy and evolution of monoaminergic systems. Am Zool 24:783–790.

Peter RE, Fryer J. 1983. Endocrine functions of the hypothalamus of actinopterygians. In: Davis RF, Northcutt RG, editors. Fish neurobiology, vol 2. Ann Arbor, MI: University of Michigan Press. p 165–201.

Portavella M, Vargas JP, Torres B, Salas C. 2002. The effects of telencephalic pallial lesions on spatial, temporal and emotional learning in goldfish. Brain Res Bull 57:397–399.

Porteros A, Arevalo R, Brinon GJ, Crespo C, Aijon J, Alonso RJ. 1998. Parvalbumin immunoreactivity during the development of the cerebellum of rainbow trout. Brain Res Dev Brain Res 109:221–227.

Probst A, Cortes R, Palacios JM. 1984. Distribution of alpha 2-adrenergic receptors in the human brainstem: an autoradiographic study using [^{3}H]p-aminoclonidine. Eur J Pharmacol 106:477–488.

Rainbow TC, Parsons B, Wolfe BB. 1984. Quantitative autoradiography of beta 1- and beta 2-adrenergic receptors in rat brain. Proc Natl Acad Sci U S A.

Randall DJ, Perry SF. 1992. Catecholamines. In: Hoar WS, Randall DJ, Farrell AP, editors. Fish physiology, vol XII, part B. San Diego: Academic Press. p 255–300.

Reiner A, Northcutt RG. 1992. An immunohistochemical study of the telencephalon of Senegal bichir (*Polypterus senegalus*). J Comp Neurol 319:359–386.

Revilla R, Fernandez-Lopez C, Revilla V, Fernandez-Lopez A. 1998. Pre- and post-hatching developmental changes in beta-adrenoceptor subtypes in chick brain. Brain Rese Dev Brain Res 111:159–167.

Rink E, Wullimann MF. 2001. The teleostean (zebrafish) dopaminergic system ascending to the subpallium (striatum) is located in the basal diencephalon (posterior tuberculum). Brain Res 889:316–330.

Rink E, Wullimann MF. 2002. Connections of the ventral telencephalon and tyrosine hydroxylase distribution in the zebrafish brain (*Danio rerio*) lead to identification of an ascending dopaminergic system in a teleost. Brain Res Bull 57:385–387.

Riters LV, Eens M, Pinxten R, Ball GF. 2002. Seasonal changes in the densities of alpha(2) noradrenergic receptors are inversely related to changes in testosterone and the volumes of song control nuclei in male European starlings. J Comp Neurol 444:63–74.

Rodriguez F, Lopez JC, Vargas JP, Broglio C, Gomez Y, Salas C. 2002. Spatial memory and hippocampal pallium through vertebrate evolution: insights from reptiles and teleost fish. Brain Res Bull 57:499–503.

Rupp B, Wullimann MF, Reichert H. 1996. The zebrafish brain: A neuroanatomical comparison with the goldfish. Anat Embryol 194:187–203.

Ruuskanen JO, Xhaard H, Marjamaki A, Salaneck E, Salminen T, Yan YL, Postethwait JH, Johnson SM, Larhammar D, Scheinin M. 2004. Identification of duplicated fourth a2-adrenergic receptor subtype by cloning and mapping of five receptor genes in zebrafish. Mol Biol Evol 21:14–28.

Ruuskanen JO, Laurila J, Xhaard H, Rantanen V-V, Vuoriluoto K, Wurster S, Marjamaki A, Vainio M, Johnson MS, Scheinin M. 2005a. Conserved structual, pharmacological and functional properties among the three human and five zebrafish α_2-adrenoceptors. Br J Pharmacol 144:165–177.

Ruuskanen JO, Peitsaro N, Kaslin JVM, Panula P, Scheinin M. 2005b. Expression and function of α_2-adrenoceptors in zebrafish: drug effects, mRNA and receptor distributions. J Neurochem 94:1559–1569.

Saidel WM, Butler AB. 1997. An atypical diencephalic nucleus in actinopterygian fishes: visual connections and sporadic phylogenetic distribution. Neurosci Lett 229:13–16.

Santer RM. 1977. Monoaminergic nerves in the central and peripheral nervous systems of fishes. Gen Pharmacol 8:157–172.

Sas E, Maler L, Tinner B. 1990. Catecholaminergic systems in the brain of a gymnotiform teleost fish: an immunohistochemical study. J Comp Neurol 292:127–162.

Scheinin M, Lomasney JW, Hayden-Hixson DM, Schambra UB, Caron MG, Lefkowitz RJ, Fremeau RT. 1994. Distribution of alpha2 adrenergic receptor subtype gene expression in rat brain. Brain Res Mol Brain Res 21:133–149.

Smeets WJAJ, Gonzalez A. 2000. Catecholamine systems in the brain of vertebrates: new perspectives through a comparative approach. Brain Res Rev 33:308–379.

Stamatakis A, Stewart MG, Dermon CR. 1998. Passive avoidance learning involves α_2-noradrenergic receptors in a day old chick. Neuroreport 9:1679–1683.

Striedter GF. 1990. The diencephalon of the channel catfish, Ictalurus punctatus. II. Retinal, tectal, cerebellar and telencephalic connections. Brain Behav Evol 36:355–377.

Subbarao KV, Hertz L. 1990. Effect of adrenergic agonists on glycogenolysis in primary cultures of astrocytes. Brain Res 536:220–226.

Svensson SP, Bailey TJ, Pepperl DJ, Grundstrom N, Ala-Uotila, S, Scheinin M, Karlsson JO, Regan JW. 1993. Cloning and expression of a fish alpha 2-adrenoceptor. Br J Pharmacol 110:54–60.

Talley EM, Rosin DL, Lee A, Guyenet PG, Lynch KR. 1996. Distribution of alpha 2A-adrenergic receptor-like immunoreactivity in the rat central nervous system. J Comp Neurol 372:111–134.

Unnerstall JR, Kopajtic TA, Kuhar MJ. 1984. Distribution of alpha 2 agonist binding sites in the rat and human central nervous system: analysis of some functional, anatomic correlates of the pharmacologic effects of clonidine and related adrenergic agents. Brain Res 319:69–101.

U'prichard DC, Greenberg DA, Sheehan P, Snyder SH. 1977. Regional distribution of alpha-noradrenergic receptor binding in calf brain. Brain Res 138:151–158.

Vanegas H, Ito H. 1983. Morphological aspects of the teleostean visual system: a review. Brain Res 287:117–137.

Wang F, Lidow MS. 1997. α_{2A}-Adrenergic receptors are expressed by diverse cell types in the fetal primate cerebral wall. J Comp Neurol 378:493–507.

Westerfield M. 1995. The zebrafish book. Eugene, OR: University of Oregon Press.

Wild JM, Williams NM, Howie JG, Mooney R. 2005. Calcium-binding proteins define interneurons in HVC of the zebra finch (*Taeniopygia guttata*). J Comp Neurol 483:76–90.

Winberg S, Nilsson GE. 1992. Induction of social dominance by L-dopa treatment in Arctic charr. Neuroreport 3:243–246.

Winberg S, Nilsson GE. 1993. Role of brain monoamine neurotransmitters in agonistic behavior and stress reactions, with particular reference to fish. Comp Biochem Physiol 106C:597–614.

Wullimann MF, Meyer DL. 1993. Possible multiple evolution of indirect telencephalo-cerebellar pathways in teleosts: studies in *Carassius auratus* and *Pantodon buchholzi*. Cell Tissue Res 274:447–455.

Wulliman MF, Mueller T. 2004. Teleostean and mammalian forebrain contrasted: evidence from genes to behaviour. J Comp Neurol 475:143–162.

Wulliman MF, Rink E. 2002. The teleostean forebrain: a comparative developmental view based on early proliferation, Pax6 activity and catecholaminergic organization. Brain Res Bull 57:363–370.

Wullimann MF, Rupp B, Reichert H. 1996. Neuroanatomy of the zebrafish brain: a topological atlas. Basel: Birkhaeuser Verlag.

Zikopoulos B, Dermon CR. 2005. Comparative Anatomy of α_2 and β adrenoceptors in the adult and developing brain of the marine teleost the red porgy (*Pagrus pagrus*, Sparidae): [^{3}H]clonidine and [^{3}H]dihydroalprenolol quantitative autoradiography and receptor subtypes immunohistochemistry. J Comp Neurol 489:217–240.

Zikopoulos B, Kentouri M, Dermon CR. 2000. Proliferation zones in the adult brain of a sequential hermaphrodite teleost species (*Sparus aurata*). Brain Behav Evol 56:310–322.

Zikopoulos B, Kentouri M, Dermon CR. 2001. Cell genesis in the hypothalamus is associated to the sexual phase of a hermaphrodite teleost. Neuroreport 12:2477–2481.

Zupanc GKH, Hinsch K, Gage FH. 2005. Proliferation, migration, neuronal differentiation, and long-term survival of new cells in the adult zebrafish brain. J Comp Neurol 488:290–319.